MATHEMATICAL MODELS OF THE TUMOR ECOSYSTEM

A Dissertation

Presented to the Faculty of the Weill Cornell Graduate School

of Medical Sciences

in Partial Fulfillment of the Requirements for the Degree of

Doctor of Philosophy

by

Kuang-Wei (William K) Chang

May 2015

MATHEMATICAL MODELS OF THE TUMOR ECOSYSTEM

Kuang-Wei (William K) Chang, Ph.D.

Cornell University 2015

The cellular composition of tumors is highly heterogeneous, involving not only divergent lineages of transformed cancer cells, but also host cells of the stroma and immune system. The complicity of protumoral host cells is essential for conferring malignancy and promoting progression in tumor in a wide range of solid tissues, including breast, pancreas, and brain. This understanding has led to the concept of ecological treatment: that is, molecular therapies aimed not directly at the destruction of cancer cells, but at disrupting interactions between tumor cells and host cells or the microenvironment, in effect creating a microenvironment unfavorable for tumor progression. In order to design effective ecological interventions and predict the course of progression of complex tumors, a quantitative understanding of the interactions between cellular subpopulations in tumors is essential. The theoretical branch of ecology has long established a history of using mathematical modeling to describe and predict the behavior of heterogeneous populations consisting of myriad interacting individuals each susceptible to noise in their responses to local stimuli, and complex systems comprised of different subpopulations engaged in asymmetrical interactions. We adapt some of these models—specifically, an agent-based self-propelled particle model and a population dynamics differential equation model—to the problems of stromal cell-dependent cancer cell migration and growth. From the former study, I find that paracrine signaling between tumor cells and increases the stability and efficiency of a preexisting tumor cell collective migra-

tion phenotype, rendering the net comigratory behavior more robust against microenvironmental fluctuations. From the latter study, I find that gliomas dependent upon protumoral tumor-associated macrophages for growth undergo multi-phasic growth dynamics. I also conclude that macrophage-targeted treatment of such tumors in a linear stage of progression leads to tumor reduction dependent on the size and composition of the tumor at the time of treatment initiation, and that tumors exhibiting weak response to such a treatment may harbor hidden vulnerability to combinatorial therapy. In addition, I infer from these theoretical studies possible methods of intervening in protumoral ecological interactions.

BIOGRAPHICAL SKETCH

William K (Kuang-Wei) "Kurtis" Chang was born in Taipei, Taiwan, and raised in, besides that city, Falcon Heights, MN; Lawrencville, NJ; and Baltimore, MD, USA. He graduated with a BA from the Biophysics Department of Johns Hopkins University in 2008, with General Honors. (It would have been Departmental Honors if he had rewritten his eventually-published manuscript [31] to fit an undergraduate thesis format, but he was too lazy to do this. He lurked enough poetry seminars that he probably could have earned a minor in Writing Seminars, had he met the foreign language requirement, but he was too lazy to do that either.) His undergraduate mentors were Rachel Green, Kalina Hristova, Greg Bowman, and Bertrand Garcia-Moreno. His undergraduate and post-graduate studies focused on structural biology of macromolecules, until he realized in the midst of a lab meeting that he really didn't care where the α-helix was. He applied to graduate school twice because he was only accepted to one PhD program the first year (see: aforementioned laziness, insouciance) and decided he didn't want to go after all.

William K moved to New York City in 2009 with the vague aim of studying emergent properties of biological systems, towards which, he dearly hopes, he has made at least *some* progress.

This PhD dissertation is dedicated to my father, Dr. Hsien-Sung Chang (3 November 1956-19 July 2002), who was a *real* doctor and wisely observed that people may not always need theoretical physics, but they will always get sick.

ACKNOWLEDGEMENTS

Thanks Mom for letting me act the prodigal son in peace for the past decade plus. Thanks Ben for taking my advice more seriously and more often than you possibly should have, and for being smarter/more talented at everything than me, which really takes the pressure off of me. (Sucks for you, though.) Sorry I haven't been around. Thanks to Uncle Scrooge for reminding me during my sophomore year of college that one professor giving me a C- in organic chemistry does not have the final word re: my future as a scientist.

To Grandma and Grandpa, I'm sorry I wasn't home for the last few years of your life. I wish you could have been around to see this.

Thanks to Keats for being with me through the second half of this whole thing and putting up with my often less-than-helpful explanations of what it is I spend all my time on.

Thanks to my cats Charlie and Yoshimi for moving to NYC with me. Couldn't have done it without your fluffy snuggles and tolerance of my frequent unreliable grad-student inability to feed you on time.

Thanks to my *de facto* sister and brother Jessica Begans and Thomas Nash for always being there, even while not physically being there, over the years and the various East Coast municipalities. And to Dr. Sarah Kolitz, who has always been one step ahead of me, telling me what was down the road.

Thanks João Xavier for being, undoubtedly, the right mentor, in the right place, at the right time. I would never have discovered my interest in collective behavior if you had not joined cBio. I am grateful for the (possibly undeserved) independence you allowed me, your constant reminders of the big questions, and it will always be my honor to have been your first PhD student. Also, thanks for the holiday parties and the mugs.

Thanks to the members of the Xavier lab, and cBio at large, past and present. In particular Silja Heilmann, Danny Parton, Karen Tkach, Poorvi Kaushner (née Kaushik), Laura de Vargas Roditi, and Sonya Hanson for their all-important friendship. Thanks also to Bobby Bowman of the Johanna Joyce lab for pretty much dropping [30] into my lap wholesale and fielding my naïve theorist questions with utmost patience.

To the members of my thesis and/or ACE committees: Johanna Joyce, Grégoire Altan-Bonnet, Richard White, and Harel Weinstein. Thanks for forcing me to keep it real and relevant, and for tabling my ACE the first try at it, which was the only thing that got my first project out of a total dead end. And to Richard, thanks so much for going above and beyond your role as faculty mentor and offering your human insight as a doctor on various matters.

Thanks to Christina Leslie, Phaedra Agius, Steve Lianoglou, Aaron Aarvey, Chris Sander, Niki Schultz, Ethan Cerami, and Barry Taylor for their help during my rotation projects, e.g. teaching me how not to blow up a computer, etc.

Finally, the work described herein would not have continued to completion without the aid of the bottomless cBio coffee machine and: Beach House, The Birthday Party, Burial, Dinosaur Jr., The Durutti Column, Fennesz, Ben Frost, Grouper, Guided by Voices, Mew, The Mountain Goats, My Bloody Valentine, Nick Cave and the Bad Seeds, Tim Hecker, Rowland S. Howard, Morphine, Max Richter, Ryuichi Sakamoto, Slowdive, Tiny Vipers...and others too numerous to mention.

TABLE OF CONTENTS

Biographical Sketch . . . iii
Dedication . . . iv
Acknowledgements . . . v
Table of Contents . . . vii
List of Tables . . . ix
List of Figures . . . x

1 Introduction to the cancer ecosystem 1
1.1 The multistage clonal sweep theory of cancer and where it got us 1
1.2 Intratumoral heterogeneity and the cancer ecosystem . . . 2
1.2.1 Heterogeneity in the cancer cell population . . . 2
1.2.2 Models of cancer cell heterogeneity . . . 3
1.2.3 Stromal cells . . . 6
1.3 Challenges of experimental studies of cancer ecology . . . 7

2 The role of mathematical modeling in cancer ecology 9
2.1 An argument of granularity . . . 9
2.2 Dynamical models . . . 10
2.3 Collective models . . . 12
2.3.1 Collective migration models . . . 15
2.4 Prior modeling studies . . . 16

3 Tumour-stromal interactions generate emergent persistence in collective cancer cell migration 19
3.1 Abstract . . . 19
3.2 Introduction . . . 20
3.3 Results . . . 23
3.3.1 Extending self-propelled particles to model a tumour-stromal interaction . . . 23
3.3.2 Rationale for values of new parameters . . . 26
3.3.3 Tumour-stromal interaction enhances collective migration in noisy environments . . . 28
3.3.4 The effect of stromal stabilization is stronger in expanding tumours . . . 31
3.3.5 Stromalized clusters are more invasive . . . 35
3.4 Discussion . . . 37

4 Withdrawal of the pro-tumoral phenotype in tumor-associated macrophages is sufficient for effective treatment of platelet-derived growth factor-driven glioblastoma in mice 43
4.1 Abstract . . . 43
4.2 Introduction . . . 44

4.3 Mathematical model and assumptions 48
4.4 Rationale of parameter values 51
4.4.1 Estimation of tumor cell population size from MRI data . 51
4.4.2 Estimation of tumor cell growth constant 53
4.4.3 Estimation of tumor cell competition constant 53
4.4.4 Estimation of educated TAM promotion constant 53
4.4.5 Estimation of max macrophage/microglia recruitment rate 54
4.4.6 Other parameters 55
4.5 Methods 57
4.6 Results and discussion 57
4.6.1 Simulations of untreated tumors 57
4.6.2 Simulations of treated tumors 60
4.6.3 Applying the model to explain BLZ945 mechanism of action in glioma mouse models 65
4.7 Discussion 69

5 Conclusions **73**
5.1 The importance of being collective 73
5.2 Proposed experimental approaches to cancer ecology and evolution 75
5.2.1 From 'big data' 75
5.2.2 From *in vivo* experiment 78
5.2.3 From *in vitro* experiment 80

Bibliography **82**

LIST OF TABLES

3.1 Parameters used in the tumor-stromal model 26

4.1 Parameters used in the tumor-macrophage population dynamics model 52

LIST OF FIGURES

2.1 Emergence of a cooperative subpopulation in a growing tumor . 14

3.1 Cancer-Stromal Model of self-propelled particles 24
3.2 Global order transition with cyclic boundary conditions 29
3.3 Phase diagram of median order in the space of density vs. noise 30
3.4 Comparison of a system with cyclic boundary conditions to an unbounded system 32
3.5 Displacement and persistence in an unbounded system 34
3.6 Stromalized clusters are larger and migrate farther in a given time 36
3.7 Stromal cells emerge as leaders of migrating clusters 40

4.1 PDG-driven glioma in mice responds to CSF-1 receptor inhibition 46
4.2 Effects of varying $\frac{T_{crit}}{K}$ on tumor growth dynamics 59
4.3 Qualitative categories of TAM-targeted treatment outcomes . . . 62
4.4 Minimum residual tumor size relative to the tumor size at time of treatment initiation in the phase space of (δ, α) 68

CHAPTER 1

INTRODUCTION TO THE CANCER ECOSYSTEM

1.1 The multistage clonal sweep theory of cancer and where it got us

The persistently dominant model of the progression of cancer on the cellular level has been that of evolution through multistage clonal sweeps [119, 112]. According to this paradigm, cancer is stochastically initiated by genomic alteration in a single cell of origin, conferring that cell and its descendent clones a selective advantage over surrounding untransformed, 'healthy' cells. This selective advantage is driven by the acquisition of one or more phenotypic markers of a set known as the *hallmarks of cancer* [86]. Such 'hallmarks' include evasion of apoptosis, unrestricted proliferation, and invasion. The tumorigenic clone would expand and generate a genomically identical descendant population. From this clonal background, one offspring cell would stochastically acquire a mutation conferring a second hallmark of cancer, rendering it more selectively fit than its peers and forebears. The clones of this cell would outcompete the other cells in the tumor and sweep through the tumor, replacing all cells in the tumor with its clones. (It was speculated that there was a sequence by which the hallmarks of cancer must be acquired, though this sequence was unknown.) This new population would then form the background for the emergence of the next generation of cancer cells expressing the third hallmark of cancer, etc., and thus drive the cancer toward increasing malignancy as the overall cancer cell population expanded locally through growth and invasion into surrounding tissue, and eventually distally through metastasis.

The multistage clonal sweep theory of cancer was generated and corroborated by, observations of homogenized tumor tissue near the end stages of the disease, when tumors become clinically detectable. At this stage, tumors display maximal malignancy and evolutionary fitness. The advent of genomic sequencing led to the discovery of mutations and copy number alterations distinguishing cancer tissue from 'normal' tissue in the same individual that were repeatedly observed across different patients of the same disease type. This resulted in a view of cancer in which each cell in a tumor possessed the full set of phenotypes necessary to drive cancer progression, and these phenotypes, in turn, were caused by a limited set of genomic alterations. Thus originated the creation of *targeted therapy*—the design of molecules that would bind to and inhibit the expressed protein products of dysfunctional genes responsible for generating the hallmarks of cancer in malignant cells. Among the best-known and most effective examples of such treatments are the treatment of chronic myeloid leukemia with Gleevec (imatinib) [49, 113] and the treatment of melanoma with BRAF inhibitors [62].

1.2 Intratumoral heterogeneity and the cancer ecosystem

1.2.1 Heterogeneity in the cancer cell population

Although capable of achieving unprecedented response with few to no side effects on short time scales, continued effectiveness of most targeted therapies are eventually stymied by regeneration of the tumor from a non-responsive, or resistant, subpopulation of cancer cells [63], suggesting the presence or devel-

opment of intratumoral cellular heterogeneity on the genomic and phenotypic levels [73].

A direct consequence of phenotypic heterogeneity can be the emergence and maintenance of a subpopulation of cancer cells that resist treatment and/or possess the capacity to regenerate the tumor mass through proliferation [137] [53]. Others may include the emergence and maintenance of a metastasis-initiating subpopulation [90]. In other words, a minority subpopulation of cancer cells could be responsible for clinically significant events such as metastasis or tumor relapse after treatment, leading to apparent resilience of the tumor even in situations where the majority of malignant cells have been neutralized by treatment or an inhospitable tumor microenvironment. Less obvious consequences of phenotypic heterogeneity among the cancer cell population can be the emergence of more complex interactions between phenotypic subpopulations and eventual construction of a 'cancer cell society' [89]: a stably heterogeneous system whose dynamics are determined by a complex network of interactions between subpopulations of cancer cells or stromal/immune cells. The dynamics of such a society of cells may be determined by cooperative [9] as well as competitive interactions.

1.2.2 Models of cancer cell heterogeneity

Within the literature, there are at least three conceptual models for how functional heterogeneity emerges in the cancer cell population. We introduce them here as the *clonal evolution* model, the *hierarchical differentiation* model, and the *phenotypic switching* model. In reality, it is most probable that all three models

have validity, and that their respective proposed mechanisms operate concurrently in any biological cancer cell population.

Clonal evolution

The first is the gene-oriented theory of clonal evolution [79]: random genomic variation emerges due to factors including the loss of genomic stability in cancer cells, sometimes known as the 'hypermutator' phenotype [106]. Fitness-conferring mutations are preserved and amplified through Darwinian selection, though they may not reach fixation due to clonal interference, cooperation, and other complex ecological relationships between clonal lineages. Clonal diversity may not emerge purely due to fitness effects: as the tumor expands in size, it is possible for different clonal lineages to segregate due to genetic drift at the expanding front. Thus, different spatial regions in a solid tumor may exhibit different genomic profiles. This phenomenon has been observed in bacterial cultures [84].

Cancer stem cells

On the other hand, even genetically identical cancer cells can differ in phenotype. One proposed mechanism for this variation is the cancer stem cell model. This model proposes that cancer cells are divided into self-renewing cancer stem cells (CSCs) and differentiated cells with limited renewal capacity. Because CSCs are not limited in the number of divisions they may undergo, though they may comprise a minority of cells in the overall cancer cell population, they may be able to regenerate the tumor after therapy has depleted the majority of differ-

entiated cancer cells [52]. Furthermore, because CSCs have unlimited renewal potential, compared with differentiated cells that are limited in the number of divisions they may perform, mutations will accumulate in the CSC compartment and propagate to the differentiated cell population.

Phenotypic switching

Phenotypic heterogeneity within a clonal population can also result from intrinsic stochastic fluctuations of intracellular regulatory networks. Huang *et al* suggested [91] that the complex regulatory networks governing cell behavior possess a finite number of attractor states, corresponding to cell fates. Intrinsic thermodynamic fluctuations within this network may drive transition between phenotypes. In agreement with this conjecture, Gupta *et al* [82] found that breast cancer cells stochastically convert between stem-like, luminal, and basal phenotypes with dynamics that can be fit to a Markov state transition model, and that each purified phenotypic subpopulation is capable of differentiating to generate the input distribution of phenotypes in culture. They also found differential susceptibility of phenotypes for chemotherapy, and predict that cells in a non-responsive state could regenerate the phenotypic repertoire post-therapy.

Phenotypic heterogeneity can also be driven by microenvironmental conditions [25, 74]. One behavior of cancer cells for which which environmentally-determined phenotypic differentiation is collective migration [97]. Cells at the leading edge of migrating cell groups are polarized by the asymmetry of integrin-mediated contact with the extracellular matrix at the leading pole versus the cadherin-mediated contact with follower cells at the trailing pole. Coordination between leader and follower cells then leads to collective motion.

1.2.3 Stromal cells

Intratumoral heterogeneity exists not only in the sense that the cancer cell population is genomically and phenotypically diverse, but in the sense that the tumor microenvironment is populated by non-transformed host tissue and immune cells. Increased resolution of the dissection of cell subpopulations within tumors has also led to the realization that not all expression of the hallmarks of cancer is autonomous to normal cells, but may be provided by host cells recruited to the tumor microenvironment [87, 85]. The participation of endothelial cells is required for neoangiogenesis [20]—the generation of new blood vessels to irrigate tumors and supply them with oxygen and nutrients—and the intravasation and extravasation processes at the beginning and end, respectively, of the metastatic cascade [165]. Immune cells perform a notably significant and diverse set of functions: for example, macrophages [120, 109, 162, 93, 123] mediate cancer growth, metastasis, and resistance to therapy. Activated tumor-associated fibroblasts can also drive the invasion of epithelial cancers [21, 70].

Though seemingly aberrant, many of the protumoral activities of host cells can be interpreted as co-opted or misdirected processes crucial for regeneration or development [45, 65]. This concept has also been expressed in the conceptualization of tumors as 'wounds that do not heal' [57]. Such mechanisms have evolved over the history of multicellular life on Earth to maintain robust function and integrity in healthy tissues in the face of unpredictable environmental perturbations [1]; naturally, they often resist attempts to disrupt or manipulate them through artificial means. To further complicate the issue, biological systems evolved for robustness often follow different 'design patterns' than artificially engineered ones [167], making the task of design effective means of

manipulating or disrupting such systems difficult.

Feedback in tumor-microenvironment interactions leads to the co-evolution of cancer cells and their environment [131]. As with many dynamical systems involving feedback interactions, the output of tumor-microenvironment interactions can be chaotic and unpredictable, as can consequences of attempts to perturb the system with conventional or targeted treatments. Thus, data taken from fixed tissue without temporal resolution will give limited insight as to how these complex interactions collectively influence disease progression.

1.3 Challenges of experimental studies of cancer ecology

Experimental dissections of the complex cancer ecosystem are necessarily limited in scope, resolution, or both. Large-scale sequencing efforts provide a comprehensive view of the genomic and transcriptomic state of the tumor, but the collection of such data via biopsy is typically invasive for solid tumors, and thus cannot provide high (if any) resolution in the temporal domain. Translating sequencing data to phenotypes relevant to the tumor population dynamics still faces difficulties.

Single-cell real-time imaging techniques can observe the morphology and behaviors of cells as well as the spatial organization of solid tumors directly. Intravital fluorescence microscopy allows *in vivo* monitoring of cell-cell interactions, and has been used to image key events in cancer invasion such as collective migration and extravasation to a metastatic site [2]. However, this technique is also invasive, with sustainable experimental duration measured in days. This may fail to capture longer-term dynamics of the tumor system, espe-

cially evolutionary events.

In vitro experiments offer benefits such as the capacity to track single cells and quantitation of signaling molecules. Microfluidic platforms are useful for imaging simple cell migration behaviors or cell-cell signaling [33]. Such assays are particularly informative in measuring the response of cells to diffusion-limited chemical signals. On the other hand, such experiments often involve cultured cell lines, which are demonstrably different from primary cells genetically and epigenetically [146]. Furthermore, as *in vitro* assays are a synthetic system—that is, they do not contain elements that have not been explicitly inserted by the experimenter—it may be difficult to capture the full scope of *in vivo* tumor complexity in an *in vitro* system.

Finally, with all fluorescence-dependent microscopy techniques, the number of microenvironmental elements that may be captured in a single experiment is constrained by the feasibility of genetic manipulation and the number of wavelengths that may be simultaneously measured. These techniques are useful for quantifying the activity of specific molecular pathways with a few known components. However, multicellular dynamics on larger time- and length-scales require integration of the outputs from vast numbers of molecular mechanisms; it is almost certain that the full long-term dynamics of a tumor rely on more molecular components than can be quantitatively imaged via fluorescence microscopy in a single assay.

CHAPTER 2

THE ROLE OF MATHEMATICAL MODELING IN CANCER ECOLOGY

2.1 An argument of granularity

Given the difficulties of experimentally capturing the full dynamic and structural complexity of tumors, it is reasonable to turn to mathematical modeling. As experiments on complex cancer behavior inevitably face an exchange of resolution for scope or vice versa, so do mathematical modeling of the same systems face a similar tradeoff of insight for complexity. To use physical terms, there is an *inverse problem* in mathematically modeling cancer progression and treatment [34]: the phenomena of interest are collective and large-scale (cancer growth, treatment, patient health), while the causal mechanisms are specific and small-scale (gene expression, cell signaling, molecular binding). Though cancer (and all complex biological systems) displays relevant behavior at all time- and length-scales—from molecular binding to the cell cycle to the development of collective tissues and neoplasms—often the modeling approach will have to be tailored to the specific scale of the phenomenon or phenomena of interest, which might be called the 'top' scale. In cancer biology, one is often also interested in the next-finer grained length scale where the driving mechanisms driving the phenomenon of interest occur, which might be called the 'bottom' scale, as this is the level at which pharmaceutical interventions may be targeted. In terms of the ecology and evolution of cancer, the relevant top scale is the dynamics of population size and composition; the finer-grained bottom scale should be the phenotypic cell-cell interactions. This latter scale is one step removed from the chemical kinetics of signaling pathways and is arguably the

appropriate bottom length scale for modeling collective cell behavior, given the variability of molecular mechanisms between and within tumors that drive similar large-scale behaviors of proliferation, invasion, and adaptation. This allows modeling the emergence of complex behavior while keeping phase space to a manageable size and increasing the generalizability of any conclusions.

The fields of statistical physics [147] and ecology [16] have long since realized the importance of the inverse problem in understanding the dynamics of complex systems constructed from large numbers of interrelated components. Theoretical methods from these fields have found applied use in fields such as sociology [127] and potentially may be of aid for solving problems in cancer biology. Below, I describe two super-classes of mathematical models in ecology that have found applications in cancer: a dynamical modeling paradigm and a collective modeling paradigm, and my extensions to them resulting in the studies presented in Chapters 3 and 4.

2.2 Dynamical models

Dynamical modeling of tumor growth has many precedents. The earliest mathematical models of tumor growth were constructed on the basis of describing the dynamics of the tumor volume [19, 36, 118]. As the tumor volume is a system-level observable, these models can be thought of as a 'top-down' approach. While useful in that they condense the phase space of tumor growth kinetics down to often just a few parameters, classical dynamics models fail to capture temporal fluctuations and spatial structure that may have a defining impact on the course of disease or diagnosis. They also typically do not account for

heterogeneity of cell populations in the tumor. Finally, even when classical models are able to reproduce the growth dynamics of real tumors, these results are often mostly descriptive, as they do not relate the bulk dynamics to parameters of cellular and molecular interactions. Thus, their capacity for inspiring novel therapeutic strategies—which usually take the form of meticulously designed and screened molecules—is inherently limited. For the purpose of studying tumor ecosystems, a mathematical model of greater detail may be desired.

An incremental generalization of dynamical models of bulk tumor growth to heterogenous cell populations is to regard it as a network of interacting subpopulations that are individually homogeneous. This can be thought of as a 'middle-up' approach. A classical example of such a model is the Lotka-Volterra model [125]. This model describes a system by the abundances of its component subpopulations, and the dynamics of the system are determined by nonlinear ordinary differential equations specifying the rates of change of each subpopulation as a function of interactions between subpopulations, or between a subpopulation and a global resource variable. The Lotka-Volterra equations can be applied to examples such as predator-prey relations or competition between species that rely on a common nutrient source.

The Lotka-Volterra model is conceptually related to models based on evolutionary game theory (EGT). In EGT models, dynamics are determined by specifying the 'payoff' of interactions between 'players,' interpretable as subpopulations. Population dynamics are then calculated from the frequencies of each interaction and their respective frequencies and payoffs of each interaction. EGT models are currently finding use in investigating events in early tumorigenesis, including how an initial minority of cancerous cells can invade a population of

normal tissue cells in homeostasis [13].

Potential uses of the Lotka-Volterra and related models in investigating cell population dynamics in cancer include competition between normal and cancerous cells for limited microenvironmental resources such as oxygen, glucose, or cytokines [25, 77]. Another application would be to explore possible outcomes of interactions between cancer cells and the systemic immune response [160, 54]. Tumor-infiltrating immune cells such as macrophages and T-cells have been hypothesized play both anti- and pro-tumoral roles [116, 109]; the net outcome of immune infiltration of tumors may depend not only on the plasticity of intracellular regulatory networks but on the dynamical balance between anti- and pro-tumoral immune subtypes. I use a Volterra-like model to explore this problem in Chapter 4.

2.3 Collective models

On the level of subpopulations, the Lotka-Volterra model is a mean-field approximation; within populations, individuals encountering different environmental conditions, or simply experiencing different stochastic fluctuations due to thermodynamic factors, may display different phenotype and behavior. The population output integrates, through interactions between individuals, the individually noisy stimuli-response calculations. These models fall under the general category of agent-based models (ABM)[170], in which collectives of interacting individuals or *agents* (e.g. cells) are simulated to observe the resultant collective behavior. These models, constituting a 'bottom up' simulation approach, have an additional advantage of being integrable with a continuum representa-

tion of diffusible chemical gradients, for example of cytokines or glucose. Such integrated models are sometimes referred to as *hybrid discrete-continuum* (*HDC*) models [4, 44]. Between the discrete-space representation of cells and their spatial organization, and the continuum representation of chemical species, HDC models have the potential to simulate the aggregate output of a multitude of regulatory mechanisms and interactions.

ABMs are useful for exploring the effect of spatial structure on population dynamics. In microbial and tissue systems, diffusive substances such as nutrients and growth factors often have a decisive effect on population dynamics. The spatial distribution of resources and individuals thus determine the dynamics of the ecosystem. For instance, spatial structure can explain the emergence and maintenance of public-goods cooperative behavior in evolving populations if cooperative individuals aggregate and the public good is spatially limited [158]. This is readily demonstrated in agent-based spatial simulations for the example of bacterial colonies [117]. Using a variant of the bacterial model, it is also possible to show the emergence of a cooperative subclone in a two-dimensional spherical tumor (Fig. 2.1). Conversely, the emergence of spatial structure can be evidence of interspecific interactions [25]. The presence of intricate spatial structure and nonuniform distribution of cell types within tumors [76, 168] may point to the dominance of interspecific effects within tumor cell populations.

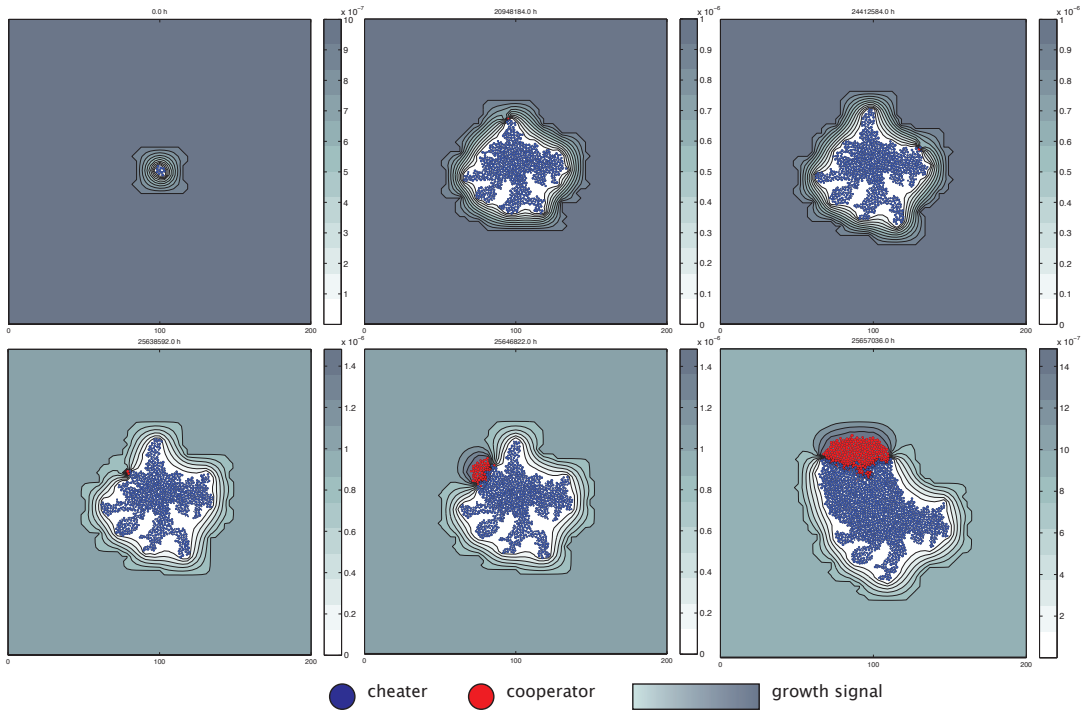

Figure 2.1: The simulation is initiated with one non-cooperative ('cheater') tumor cell at the center of the simulation space. Growth signal is initially uniformly distributed throughout the space, but gradients emerge as the signal is consumed by growing cells. Stochastic emergence of a cooperative subtype, which expresses the growth signal at a cost to its own growth, at the edge of the expanding tumor leads to a locally high concentration of growth signal and overall acceleration of cell growth. The emergent spatial structure—aggregation of cooperators and consequent segregation of public goods—stabilizes the cooperative subpopulation.

2.3.1 Collective migration models

One problem in which agent-based models have proven useful in studying is the phenomenon of collective motion. Biological organisms at all scales ranging from bacteria to mammals exhibit coordinate motion between individuals in a group, and similar phenomena can be observed even in inorganic systems [157]. Much of the work done in this field—investigating how collective patterns of motion arise from signaling or mechanical interactions between moving individuals—has been performed using a special instance of agent-based models known as the *self-propelled particle (SPP)* model [156]. Simulations using the basic SPP model show that a system of moving individuals can exhibit discontinuous changes in qualitative behavior—better known as a *phase transition*—as the parameters governing the response of individual particles and the density of particles are continuously varied. Extensions of this model have been used to investigate biological questions such as cell sorting during development [17, 11].

These existing studies have been primarily inspired by theoretical physics and applied to problems in developmental biology and microbiology, with a focus on critical phenomena—that is, qualitative changes of behavior resulting from fine tuning of parameters within a narrow range of values. In cancer biology, collective migration often emerges as a consequence between phenotypically distinct cells originating from separate lineages of differentiation. In Chapter 3 I present an application of this model to the emergence of collective comigration from interspecific signaling between cancer cells and stromal cells such as tumor-associated macrophages.

2.4 Prior modeling studies

Recently, the primary approach to mathematical modeling the cancer ecosystem has been a mechanistic or quasi-mechanistic focus on integrating individually-known signaling pathways in an attempt to comprehensively simulate the aggregate impact of many specific molecular species, or categories of molecules and mechanisms, on tumor progression. These efforts seem to have emerged as a attempt to reconcile the increasingly-overwhelming body of The parameters of these models usually correspond to kinetic rate parameters of specific biochemical signaling pathways and cell mechanisms inferred either from isolated measurements of signaling molecules in controlled cell-biological experiments [5], or literature reporting the same. Such models are often implemented in spatially structured simulations; in this form, they can serve as a kind of augmented *in vitro* experiment, serving as an alternative to spatially-unstructured conventional cell line experiments. One prominent example of such a model is the hybrid discrete-continuum (HDC) model developed by Anderson *et al* [6]. In this study, the authors observed that a harsh simulated tumor microenvironment promotes the evolution of invasive tumor cell clones, while a mild microenvironment enabled less invasive clones to persist and suppress the emergence of invasive cells through clonal competition.

Integrative mechanistic models can also be conceived as mean-field, differential equation models. In [162], the authors implemented a glioma model of 5 tumor and stromal cell types, 15 cytokines, and 69 signaling pathways, and observed that the simulated tumor developed in dynamically and compositionally distinct pre-tumoral, expanding, and saturated stages. They further discover that treatment depleting microglia is effective for treating such tumors in the

early stages, but in the late stages cytokine inhibition is required.

These studies show the potential of integrative, mechanistic or quasi-mechanistic approaches to modeling cell-cell and cell-microenvironment interactions in cancer can predict emergent properties of the tumor that would be challenging to experimentally obtain. In addition, by grounding the model in detailed molecular and mechanistic knowledge, such models can propose novel therapeutics.

The major challenge with mechanistic and quasi-mechanistic modeling studies is that the complexity of the model increases rapidly as the number of signaling mechanisms represented increases, often making numerical simulation the only tractable analysis of the model. It is difficult to parameterize such a complex model. Often reference to literature or experiments measuring stimuli-response cell dynamics under simplified culture systems, for example, will be required. However, it cannot always be guaranteed that such dynamics will remain quantitatively consistent when combined with other mechanisms in a complex experimental or simulated environment. Additionally, the significance of any interaction or parameter then becomes difficult to disentangle from the context of every other interaction and parameter in the system, and in cases where a specific effective perturbation of the system cannot be readily identified from simulation outputs, extracting useful insight from the model becomes a challenge.

Phenomenological modeling has been less prominent in recent years, due to their abstraction and the dominance of molecular biology. One remarkable exception can be found in a study by Leder *et al* [103]. In summary, the authors constructed a simple population dynamics model integrating phe-

notypic switching between radiation-sensitive and -resistant states in PDGF-driven glioma cells. The model was parameterized from MRI experiments and literature, and a Monte Carlo optimization algorithm was used to propose a radiation dosing schedule to minimize the number of residual tumor cells two weeks after conclusion of treatment. The resulting novel treatment strategy was tested in a mouse model and found to provide improved response compared to the standard clinical dosing schedule. This study is a prominent recent example of how non-mechanistic models, working in correspondence with experimentation towards a well-defined optimization endpoint, can yield biologically significant results.

On the other hand, this type of modeling approach amounts to a parameter optimization problem, one of peculiar clinical relevance, and is tightly bound with a specific set of conventional biological experiments. Therefore, the generality of the modeling results, or their applicability to other biological systems, may be difficult to know *a priori*. More abstract, parameter-independent approaches may be preferable if the goal is rather to illuminate the general principles of multicellular dynamics in tumors.

CHAPTER 3

TUMOUR-STROMAL INTERACTIONS GENERATE EMERGENT PERSISTENCE IN COLLECTIVE CANCER CELL MIGRATION

This chapter has been previously published as [29].

3.1 Abstract

Cancer cell collective migration is a complex behaviour leading to the invasion of cancer cells into surrounding tissue, often with the aid of stromal cells in the microenvironment, such as macrophages or fibroblasts. Although tumour-tumour and tumour-stromal intercellular signaling have been shown to contribute to cancer cell migration, we lack a fundamental theoretical understanding of how aggressive invasion emerges from the synergy between these mechanisms. I use a computational self-propelled particle model to simulate intercellular interactions between co-migrating tumour and stromal cells and study the emergence of collective movement. I find that tumour-stromal interaction increases the cohesion and persistence of migrating mixed tumour-stromal cell clusters in a noisy and unbounded environment, leading to increased cell cluster size and distance migrated by cancer cells. Although environmental constraints, such as vasculature or extracellular matrix, influence cancer migration *in vivo*, our model shows that attractive cell-cell interactions are sufficient to generate cohesive and persistent movement. From our results, I conclude that inhibition of tumour-stromal intercellular signaling may present a viable therapeutic target for disrupting collective cancer cell migration.

3.2 Introduction

One of the most harmful features that tumour cells acquire is the ability to migrate and invade surrounding tissues, leading to deadly systemic metastases [64]. This has fueled an active research programme to understand cancer cell migration and invasion from experimental and theoretical points of view. Novel techniques for direct visualization of tumour invasion *in vivo* [38] have revealed that cancer cells frequently migrate as groups of closely interacting cells [67]. The phenomenon of collective cell migration also emerges in a broad range of 'normal' physiological conditions ranging from embryonic development to wound-healing [139]. However, we still lack a complete and thorough understanding of how individual cells coordinate to migrate collectively.

Ecological models may be useful in understanding cancer collective migration. Collective migration is observed in biological systems of many disparate length scales, ranging from bird flocks [157, 122, 28] to bacterial swarms [41, 42]. It is an emergent phenomenon and a universality class, in which the large- scale properties of the collective result from the activities of individuals, but are to some extent independent of the specific behaviour of individuals [152, 95]. Similarly, in cell biology, collective migration of groups of closely interacting cells has been implicated in such behaviours as organ morphogenesis during embryonic development or vascularization [139, 26, 65, 149, 128] and, the main motivation for our study, cell invasion during cancer progression [48, 65].

One of the most successful theoretical approaches to study the emergence of collective migration from simple interactions between moving individuals are a class of models called self-propelled particles (SPPs). In the classic SPP model

[156] an individual moving at a fixed speed interacts with its neighbours by aligning itself with the average direction of all individuals within a given radius. These simple rules for local interaction give rise to emergent global properties, such as a phase transition from disordered, or individual, motion to ordered, or collective, motion with a decreasing level of noise in the interaction. This model and derivations of it have been applied to numerous problems in collective migration by using the individual particle to represent real-world individuals in collectives, such as an animal in a flock [40, 138], micro-organisms in a colony [18] or a cell in a tissue [94, 150].

Experiments in which a homogeneous cell population displays collective migration in the absence of other cell types or external signals [27, 66, 88, 150] are compatible with the original SPP model. However, migratory cancer cells interact not only with each other but also with stromal cells. For example, stromal cells such as macrophages [93, 134] and fibroblasts [70] are known to assist cancer cell migration through secretion of migration-stimulating cytokines and proteinases that remodel and create permissive tracks in the extracellular matrix [64, 140]. Thus, the application of the SPP model to cancer is complicated because cell migration in tumours requires synergy between diverse cell types [37, 78, 140]. The SPP paradigm has been used before to investigate cell sorting in development and regeneration [11, 17]. However, application of the SPP to investigating migration emerging from heterotypic and non-reciprocal interactions between distinct classes of motile cells has been limited, though some examples exist [17].

Here, I explore what are the consequences of implementing experimentally inspired modifications to the original SPP model. More specifically, I inves-

tigate what are the consequences of the presence of a small subpopulation—representing stromal cells—with a distinct behaviour. Thus, I extend the Vicsek SPP algorithm [156] to introduce an additional particle type representing stromal cells. Tumour-associated macrophages are one of the most abundant and well-studied stromal cell types within solid tumours [134]. These macrophages are known to attract cancer cells, and this interaction is crucial for tumour invasiveness *in vivo* [140, 164, 166]. Based on these observations, I add a specific non-reciprocal attraction rule compelling cells of one type (tumour) towards nearby cells of the second type (stromal). This attraction has a relatively longer range of action, i.e. can occur between non-adjacent cells. I use our expanded model (hereafter referred to as the cancer-stromal model) to explore cell displacement and cell cluster size as metrics for quantifying the impact of stromal cells on collective cancer cell migration. Our simulations suggest that stromal cells can have profound implications for large-scale cancer cell collective migratory patterns and, consequently, for tumour aggressiveness.

It is important to stress that, although our initial motivation is to model attractive macrophage-tumour interactions described experimentally [140, 164, 166], our model is simplified and neglects other aspects of cancermacrophage interaction such as angiogenesis promotion [108, 126] and modulation of the inflammatory response [39]. We also note that our simulations occur in an unstructured space. In other words, the results of our model should be interpreted as the intercellular signaling component of collective cell migration, removing the effects of tumor microenvironmental structure. In summary, the model is general and can be extended to any other attractive stromal cell. Expansions of model features can be made to account for noncellular elements of the tumor microenvironment.

3.3 Results

3.3.1 Extending self-propelled particles to model a tumour-stromal interaction

We use the homogeneous population of SPPs with one simple alignment rule as described in the original SPP model [156] as a starting point to model migrating tumour cells. To this population, we introduce a minority population of a second type of SPP, representing stromal cells. Cells of both kinds, tumour or stromal, align non-specifically to the mean polarization of cells in the neighbourhood. In addition, we add an attractive tumour-stromal interaction. This interaction is assumed to be type-specific and asymmetrical, that is, tumour cells are attracted to nearby stromal cells, but not vice versa (Fig. 3.1A). The angle of polarization θ of each cancer cell i is thus recalculated at each iteration:

$$\theta_i t + 1 = \langle \theta(t) \rangle_{ral} + a_{ts} \langle \arg(\vec{r}_{ij}) \rangle_{rts} + \Delta\theta \tag{3.1}$$

where $\theta(t)_{ral}$ is the mean angle of polarization of all cells within distance r_{al} of the focal tumour cell i; a_{ts} is the strength of the attractive tumour-stromal interaction relative to cell-cell alignment; $\arg(r_{ij})$ is the mean angle of vectors from the centre of focal tumour cell i to all stromal cells j within distance r_{ts} of cell i; and $\Delta\theta$ is a random angle on the interval $[-\eta, \eta]$, representing noise. The polarization calculation for stromal cells lacks the second term, and thus is identical to the migration rule in [17],

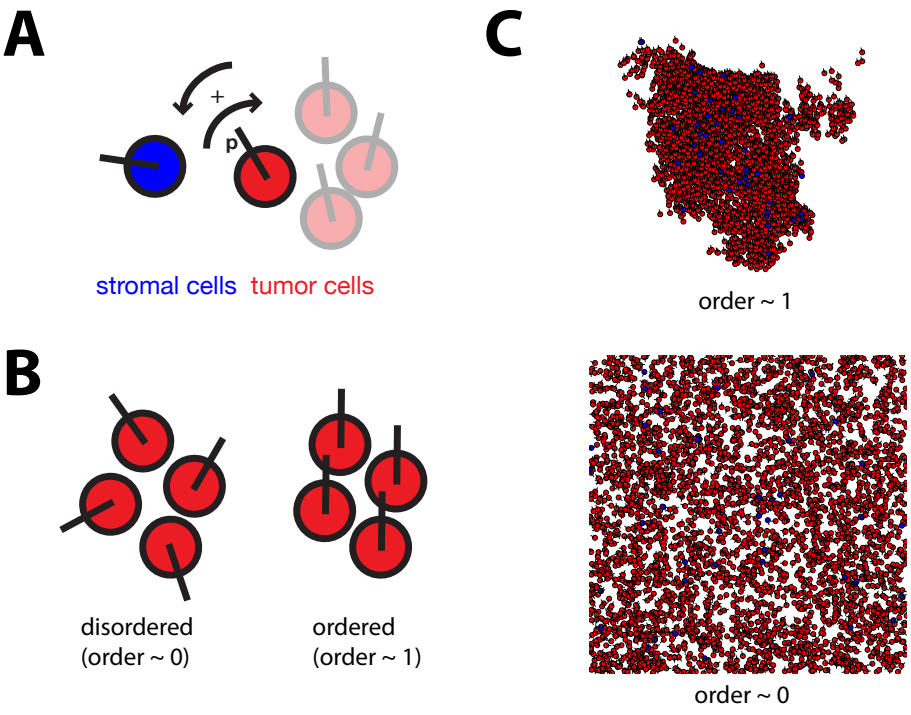

Figure 3.1: A) Cell-cell interactions in the Cancer-Stromal Model of self-propelled particles. Cells move at fixed speed. Stromal cells align nonspecifically to local mean direction of motion. Tumor cells align nonspecifically in addition to moving towards any nearby stromal cells. p represents the polarity of cell motion. B) Order parameter quantifies the extent of cell polarization. When the global order parameter is ≈ 0, cells are randomly polarized. When the global order parameter is ≈ 1, cells are polarized in the same direction. C) In a system with no tumor-stromal attraction ($a_{ts} = 0$; i.e. all cells behave as tumor cells) with low noise and cyclic boundary conditions, in the infinite-time limit, the global order parameter approaches 1: almost all cells eventually group into a single coherent cluster, where individual polarizations deviate little from the mean polarization of the cluster. In a high-noise system, the global order parameter approaches 0, and the cells are spread throughout the available space with no discernible clustering.

$$\theta_i(t+1) = \langle\theta(t)\rangle_{ral} + \Delta\theta \tag{3.2}$$

All length scales and cell speeds in the model are normalized as previously [156]: that is, the range of cell-cell alignment, r_{al}, equals 1. Local interaction mechanisms such as cell- cell adhesion and shear viscosity at high cell density [151] can account for this short-range alignment.

Conversely, we assume that the possible mechanisms for tumour-stromal interaction, such as paracrine signaling through diffusible molecules [140, 164], chemotactic motility from cancer cells towards stromal cells or forms of long-range alignment via adhesion to common collagen fibres in the extracellular matrix [64, 140], have greater effective range than those contributing to cell-cell alignment adhesion to common collagen fibres in the matrix [64], and set $r_{ts} = 2$. Interaction and noise strengths are normalized to the cell-cell alignment strength; that is, cell-cell alignment strength equals 1. The noise amplitude, η, varied from $0 \leq \eta \leq 5$, which is the range in which the ordereddisordered phase transition was observed previously [156], and the interaction strength, a_{ts}, varied from $0 \leq a_{ts} \leq 2$.

All simulations were performed in two dimensions, replicating the cell density and boundary conditions, again as used previously [156]. We used a ratio of 4000 simulated tumour cells and 40 simulated stromal cells. With $a_{ts} = 0$, the stromal cells effectively behave identically to the tumour cells and the model should be equivalent to the original SPP. Our cancer-stromal model, when its additional parameters are set to 0, thus reproduces the behaviour previously observed in the original SPP study [156]. Simulation parameters are summarized in Table 3.1.

parameter	*value*	*rationale*
cell migration speed	0.03	as in [156]
size of simulation space	31.6×31.6	as in [156]
range of cell-cell alignment	1	as in [156]
strength of cell-cell alignment	1	as in [156]
noise	$0 \leq \eta \leq 5$	as in [156]
number of cancer cells	4000	as in [156]
number of stromal cells	**40**	See 3.3.2
range of tumor-stromal attraction	$\boldsymbol{r_{ts} = 2}$	See 3.3.2
strength of tumor-stromal attraction	$\boldsymbol{a_{ts} = [0, 0.2, 0.4, 0.6, 0.8, 1.0, 2.0]}$	See 3.3.2

Table 3.1: Parameters used in the tumor-stromal model. Parameters not in the original SPP model [156] are highlighted.

3.3.2 Rationale for values of new parameters

- *Number of stromal cells*. We initially performed simulations with a small minority of stromal cells (1 in 100) to perturb the system minimally. When this small subpopulation proved to have significant effect on the population-level collective migration performance, we used this stromal ratio for all simulations. From fluorescent cross-section data in e.g. [133], one can infer the bulk relative abundance of macrophages in late-stage solid tumors (glioma in this case) as being approximately 10-20%. However, this does not distinguish between macrophage phenotypes, or microenvironmental variability affecting the role individual macrophages play in interactions with the local tumor cell subpopulations. It is important to note that in unbounded simulations, because of the heterogeneity generated by cell dispersion, effective stromal cell ratio per interconnected

cell cluster varies greatly (from 0% to 100%), and thus the global stromal cell ratio does not have direct biological translation.

- *Range of tumor-stromal attraction (r_{ts}).* We assume that cell-cell alignment occurs through either direct contact-based E-cadherin-mediated coupling through adherens junctions or mechanical shearing. The normalized alignment range ($r_{al} \equiv 1$) can thus be thought of as the radius of a single cell. The tumor-stromal interactions are assumed to represent paracrine signals, such as the well-documented EGF/CSF-1 paracrine signaling loop between breast cancer cells and tumor-associated macrophages [78]. As such, they are expected to have a longer effective range, but still within the same order of magnitude in terms of cell lengths, as contact-mediated interactions [15]. An effective interaction length of $r_{ts} = 2$ satisfies this constraint. Though we did not experiment with different values of r_{ts}, one can speculate that this will have qualitatively a similar large-scale effect as reducing the noise, and thus increasing the effective distance by which the tumor-stromal interaction signal can be propagated by interactions between cancer cells. That said, experimenting with changes in r_{ts}, or performing dimensional reduction to generate a model that is independent of the specific value of r_{ts}, could be an interesting direction for future research.

- *Strength of tumor-stromal attraction (a_{ts}).* The strength of the tumor-stromal attraction is defined relative to the strength of cell-cell alignment with a_{ts} as the scaling factor. We experimented with a range of values for a_{ts}, ranging from 'control' simulations with no tumor-stromal attraction ($a_{ts} = 0$)

to attraction twice as strong as alignment ($a_{ts} = 2$). There was no significant variation in the population-level behavior, and for simplicity we fixed $a_{ts} = 1$ for subsequent simulations.

3.3.3 Tumour-stromal interaction enhances collective migration in noisy environments

We first evaluated whether our model performed behaved consistently by calculating the global order parameter, a key parameter in the original SPP model [156]. Briefly, the order parameter quantifies the average direction of particles, which we then compared at the pseudo-steady state (10000 iterations) with the results in the original study. As expected, a global order parameter of ≈ 0 indicates a disordered system with cells randomly polarized and distributed throughout the simulation space, while a global order parameter of ≈ 1 indicates a system where all the cells are roughly aligned and migrating as a single coherent cluster (Fig. 3.1B-C). A phase transition from ordered to disordered motion occurred as η increases. These observations confirmed that our SPP implementation corresponded to the original model [156].

We then considered the effect of tumor-stromal attraction on the order of motion by setting a_{ts} to positive values. Simulations with $a_{ts} > 0$ showed notable deviations from the original SPP model [156]. We observed high variability in global order at the end of the simulation runs, but with opposite trends for low and high noise. The global order decreased compared to $a_{ts} = 0$ for low values of $\eta (\eta < 2.5)$, and increased for high values of η ($\eta \geq 3$, Fig. 3.2). End-simulation

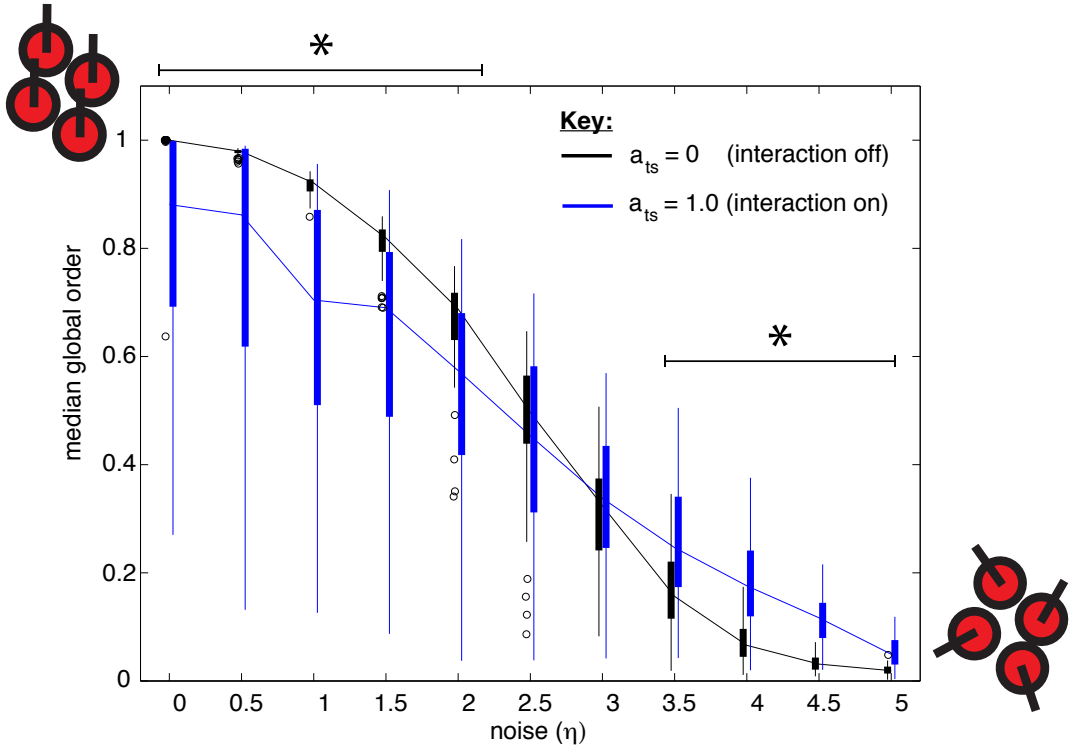

Figure 3.2: Global order parameter as a function of noise in a system with cyclic boundary conditions. Under a fixed value of a_{ts}, as η is increased, the system exhibits a phase transition from an ordered (global order parameter ≈ 1) to disordered (global order parameter ≈ 0). When $a_{ts} = 0$, the phase transition occurs as in ref. 14. When $a_{ts} = 1.0$, global order is decreased for low values of eta, but increased for high values of eta compared to the $a_{ts} = 0$ system. Asterisks indicate significant difference between the $a_{ts} = 1.0$ and $a_{ts} = 0$ simulations ($p < 0.001$).

global order did not noticeably vary between simulations with different positive values of a_{ts} and the same value of η (not shown). The effect of changing cell density simultaneously with noise on the phase diagram of the order parameter is shown in Fig. 3.3.

These results demonstrate that a simple extension to the original SPP can produce a significant change in the predicted pattern of collective migration and may have important implications for cancer. Specifically, the results suggest

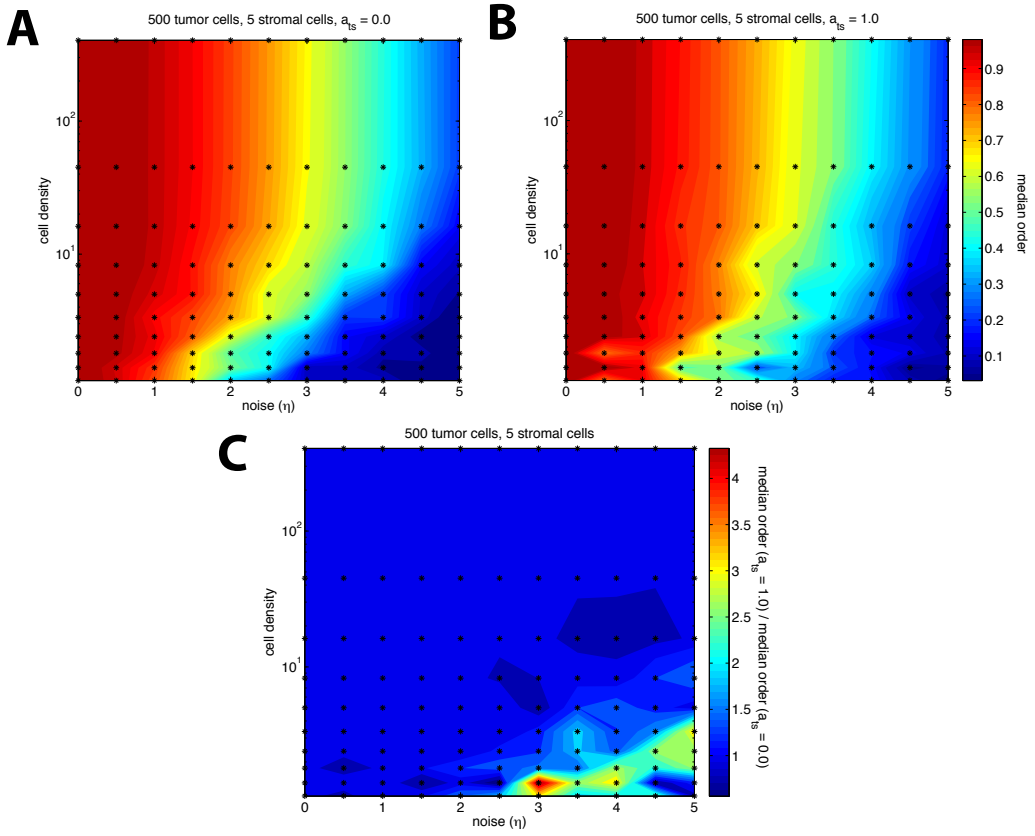

Figure 3.3: A) Phase diagram of the median order parameter in the space of density vs. noise for $a_{ts} = 0$. Asterisks (*) represent data points (5 replicates each); colors are filled using bilinear interpolation. B) Same as A), for $a_{ts} = 1$. C) Ratio of values in B) to values in A). This shows that the positive effect of tumor-stromal interaction on the order can mainly be seen in the regime of medium to high noise, with the critical noise threshold increasing with cell density. Notably, the effect is most observable within the range of densities used in [156].

that tumor-stromal interaction can stabilize cancer collective migration in noisy systems.

3.3.4 The effect of stromal stabilization is stronger in expanding tumours

Our model so far, like the original SPP model, assumes cyclic boundary conditions [156], which confine the particles to a space of torus-like geometry and unrealistically small volume. However, cancer invasion *in vivo* drives cancer progression on time and length scales much larger than those of individual cell migration or even intercellular signaling within small groups of cells [5]. To extrapolate collective co-migration of cancer and stromal cells to larger length scales and longer simulation times, we implemented a second extension in our model, now using an unbounded system where cell migration is essentially unlimited by spatial constraints (Fig. 3.4A).

We carried out simulations with the unbounded system for a range of interaction strength and noise levels and we calculated the global order parameter after 10000 time steps. As expected, with no tumor-stromal interaction ($a_{ts} = 0$), the global order decreases towards end of simulation for all levels of noise (Fig. 4.3B). This occurs because in unbounded systems, the decoherent effect of noise in each cell cluster is cumulative, and unlikely to be cancelled by encounters with other cell clusters; thus, the ability of the system to sustain large coherent clusters over long time spans is decreased. Adding tumor-stromal interaction uniformly increases the end-simulation global order for all noise levels, implying that tumor-stromal interaction has much greater impact on the coherence of migrating cancer cell groups when the available space is large. Tumor-stromal interaction delays the disintegration of coherent migrating clusters, and increases the end-simulation global order (Fig. 3.4B).

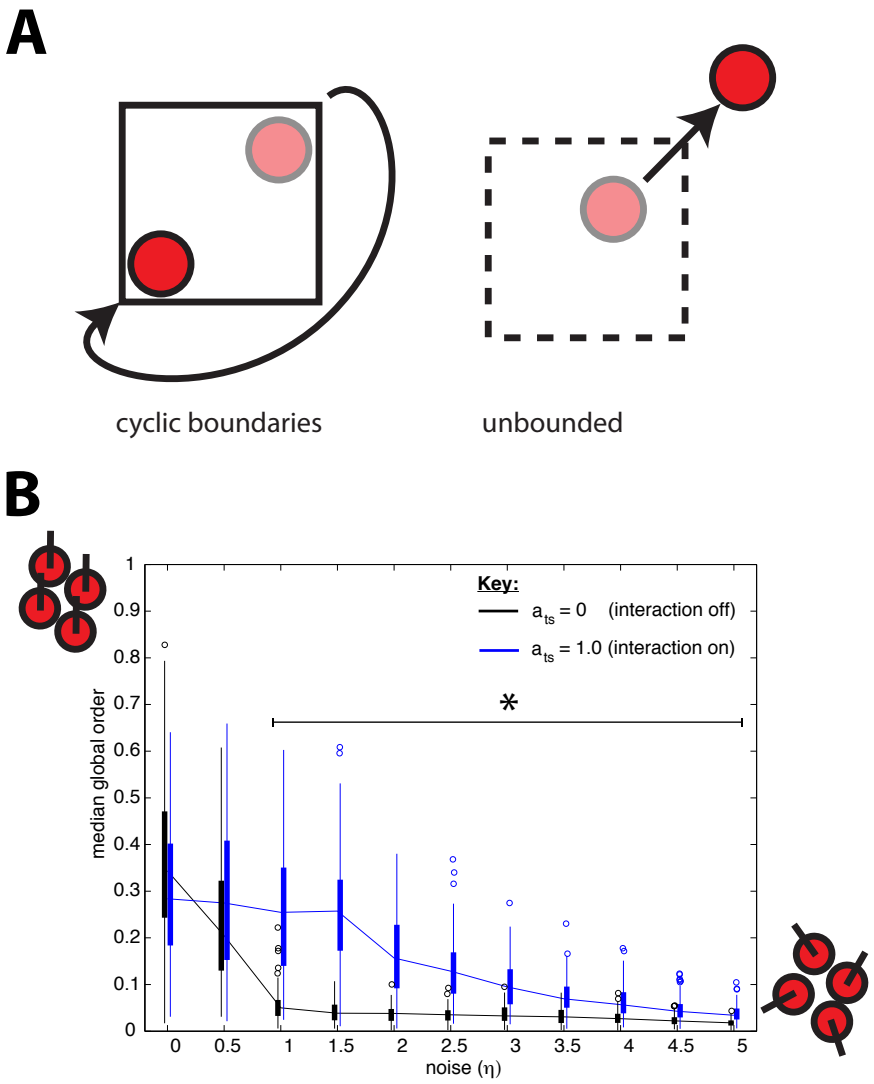

Figure 3.4: Comparison of a system with cyclic boundary conditions to an unbounded system. Squares indicate areas of inoculation. In a system with cyclic boundary conditions, cells leaving the area of inoculation will re-enter the area at the diametrically opposite point, maintaining its polarization. In an unbounded system, the cell is not spatially constrained and may leave the area of inoculation. B) Global order parameter as a function of noise in an unbounded system. The order of the system decreases rapidly as eta increases. When $a_{ts} = 1.0$, the order increases for all positive values of eta compared to simulations where $a_{ts} = 0$. Asterisks indicate significant difference between the $a_{ts} = 1.0$ and $a_{ts} = 0$ simulations ($p < 0.001$).

In addition to calculating the order parameter, we also examined the distance migrated by cancer cells as a measure of cancer cell invasiveness. For simulations without tumor-stromal interaction where noise is moderate to high, the mean displacement rapidly increases initially but starts to level off within the simulation time (Fig. 4.4A). In contrast, in simulations with tumor-stromal interaction, the mean displacement increases steadily (linearly) throughout the duration of the simulation; this increase is seen to saturate within the simulation time only when noise levels are high (Fig. 3.5A). Consequently, for all positive values of η tested, tumor-stromal interaction increased the mean distance migrated by cancer cells (Fig. 3.5B). We conclude that tumor-stromal interaction increases the persistence and ultimately the performance of collective cancer cell migration, as measured by distance travelled.

We also considered the effect of tumor-stromal interaction on the size of collectively migrating cell clusters, as measured by the number of cells in the clusters. Clusters are defined as groups of cells within the same interaction network, i.e. cells interacting directly or indirectly via other cells. We determined the presence of cell-cell interactions by thresholding the center-center distance of each pair of cells with the appropriate interaction range (1 for a pair of tumor cells or a pair of stromal cells, 2 for a heterogeneous pair of 1 stromal cell and 1 tumor cell) and sorted the cells into clusters using the well established equivalence class sorting algorithm [132]. Stromal cells were included in the statistics for their respective clusters; however, as they constituted 1% of the total population, we assumed they did not significantly affect the overall statistics. Cells not in contact with another cell were interpreted as clusters of size 1. At low levels of noise, tumor-stromal interaction increased the global mean size of collectively migrating cell clusters compared to the control simulations.

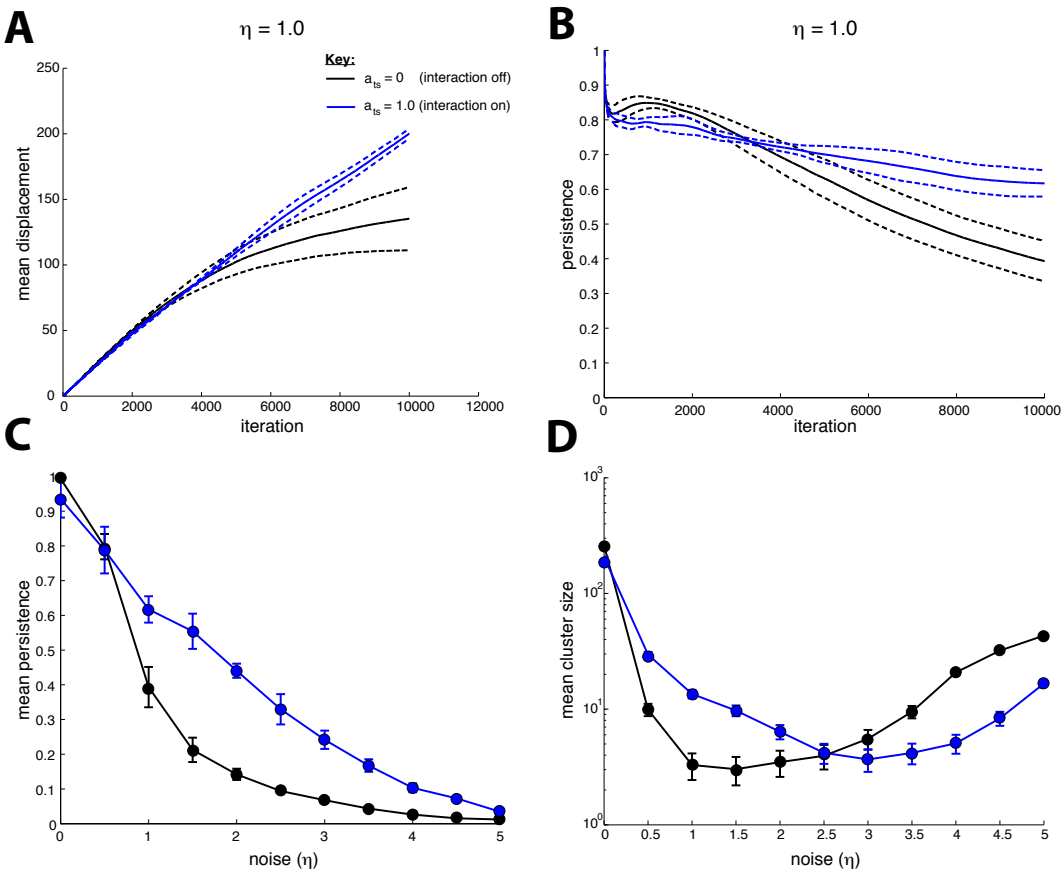

Figure 3.5: A) Time course of mean displacement of cells in the system. Dashed lines indicate standard deviation across 5 replicates. The mean cell displacement at end of simulation is increased for $a_{ts} = 1.0$ when compared to $a_{ts} = 0$. In the $a_{ts} = 0$ simulations, the rate of displacement increase decreases over time, whereas the effect is not observable in the $a_{ts} = 1.0$ simulations. B) Persistence over time of the same simulation sets. The decay of persistence over larger time scale is more gradual for $a_{ts} = 1.0$. C) Mean persistence over the time scale of the simulation as a function of noise. The mean persistence is increased for $a_{ts} = 1.0$ compared to $a_{ts} = 0$ for all values of $\eta > 0$ tested. D) Mean cluster size at simulation end as a function of noise. The mean cluster size is increased for $a_{ts} = 1.0$ at low values of noise. At high levels of noise, tumor-stromal interaction decreases the mean cluster size, reflecting the dissolution of the cell population into small clusters.

However, this trend reversed as η was increased above approximately 2.5, and for high levels of noise, tumor-stromal interactions in fact decreased the global mean cluster size (Fig. 3.5C).

3.3.5 Stromalized clusters are more invasive

To understand this biphasic effect of tumor-stromal interaction on the sizes of migrating clusters (Fig. 3.5C), we then sorted the cell clusters into those included at least one stromal cell ('stromalized' clusters) and those that were not ('unstromalized' clusters) (Fig. 3.6A). We estimated the distance migrated by a cluster of interacting cells by calculating the mean displacement of all cells in the cluster at end of simulation. We then examined the relationship between the stromalized cluster, the distance it migrated by a cluster, its stromalization status, and its size. In the low-noise ($\eta \leq 0.5$) regime, both the stromalized and unstromalized clusters were smaller and displayed a smaller mean displacement than clusters in the control $a_{ts} = 0$ simulations (Fig. 3.6B). This is caused by the same fragmentation and consequent decrease in coherence observed in the cyclic boundary simulations. In addition, the distribution of multiple stromal cells throughout the cell population at inoculation possibly creates multiple conflicting directional signals that propagate through many cancer cells, leading to wandering behavior that contributes little to the mean displacement.

For larger values of η, both the size of and distance migrated by clusters decreases noticeably for the control simulations. The stromalized clusters separate into a distinct coherent, far-migrating subpopulation (Fig. 3.6C). At very high noise levels, cluster size and distance migrated are decreased for both stromal-

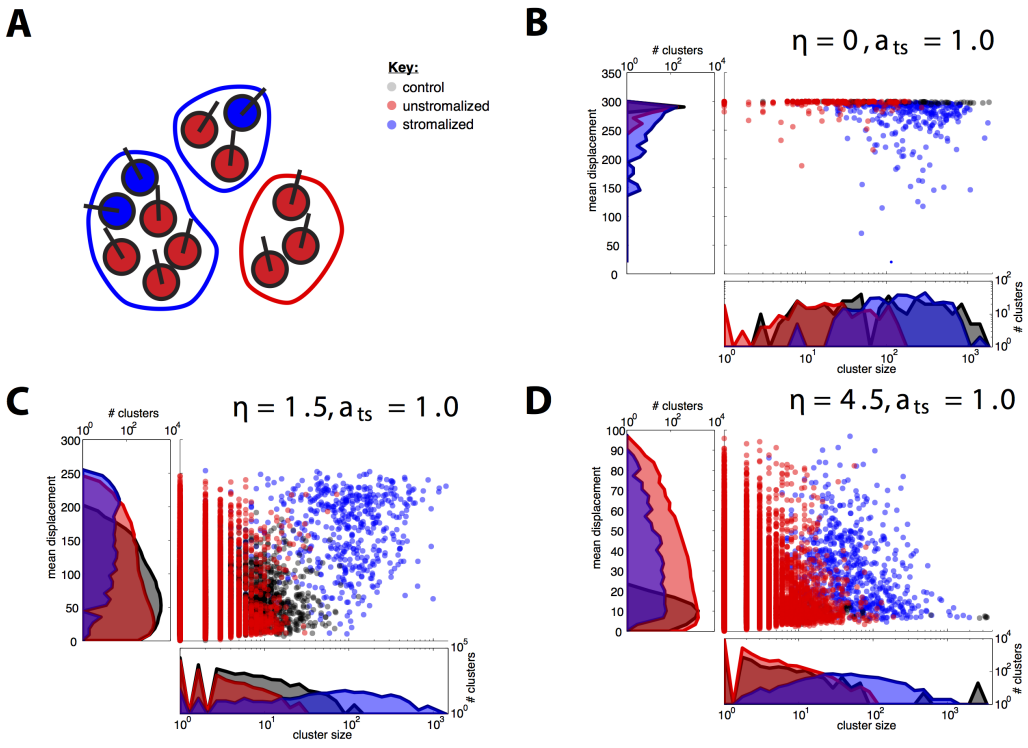

Figure 3.6: A) Clusters incorporating at least one stromal cell are considered stromalized. B) Distributions of cluster sizes and displacements for stromalized and unstromalized clusters in 5 test simulations ($a_{ts} = 1.0$) versus control ($a_{ts} = 0$) for a low-noise condition. Clusters in the control simulations varied in size but are uniformly far-migrating. In the test simulations, stromalized clusters tended to be larger than unstromalized clusters, though they showed greater variance in displacement. C) Distributions of cluster sizes and displacements for stromalized and unstromalized clusters in 5 test simulations ($a_{ts} = 1.0$) versus control ($a_{ts} = 0$) for a medium-noise condition. Unstromalized clusters in test simulations distributed similarly to clusters in control simulations both in terms of size and displacement. Stromalized clusters in test simulations distributed distinctively from the unstromalized and control clusters, displaying greater displacement and cluster size overall. D) Distributions of cluster sizes and displacements for stromalized and unstromalized clusters in 5 test simulations ($a_{ts} = 1.0$) versus control ($a_{ts} = 0$) for a high-noise condition. Stromalized and unstromalized clusters from the test simulations distributed similarly with respect to displacement, with stromalized clusters being larger overall. Cells in the control simulations formed large, nonmotile clusters due to being unable to significantly migrate from their points of origin. In the test simulations, tumor-stromal interactions break the cells into small, motile clusters.

ized and unstromalized clusters in test simulations, and for all clusters in control simulations. Regardless, stromalized clusters retain a significantly larger mean cluster size than the unstromalized subpopulation (Fig. 3.6D). These results suggest that tumor-stromal interaction can increase both the motility of migrating cancer cells and the number of motile cancer cells.

Notably, control simulations saw the emergence of very large clusters, on the order of 1000 cells, with cluster displacement close to 0 (Fig. 3.6D). This is because the cells are inoculated at high enough density to constitute a single interacting cluster, and at high noise, most cells are unable to 'escape the inoculum cluster. Similarly to the medium-noise situation, these results suggest that in microenvironments that present strong barriers to cancer cell migration, interaction with stromal cells can aid in the escape of motile cancer cells from the main tumor mass.

3.4 Discussion

In order to understand the effect of complex tumor-stromal and tumor-tumor intercellular interactions on collective cancer cell migration, we have implemented and analyzed the Cancer-Stromal model, a minimal computational model for simulating the collective co-migration of two phenotypically distinct cell types under the SPP paradigm. We have designed the model with intended application to stromal cell-assisted cancer cell invasion, but it can theoretically applied to any heterogeneous population where interaction between subpopulations is orthogonal to interaction within subpopulations, for example a symbiotic or antagonistic relationship between two animal herds of different species.

We find that, given an unbounded space in which to disperse, the addition of tumor-stromal interaction increases the end displacement of cells within stromalized clusters. The presence of system-level effects in our simulations is remarkable, considering the stromal cells constitute < 1% of all cells in the system, and in an unbounded system only a slim minority of cancer cells will directly interact with stromal cells in the course of a simulation.

The effect of tumor-stromal interactions on the sizes of co-migrating cell clusters changes relative to the amount of noise in the system. At finite but low levels of noise, positive attraction between tumor and stromal cells increases the size of stromalized clusters over unstromalized clusters in the same system, or clusters in systems where tumor-stromal attraction is absent. With high levels of noise, cancer cells tend to clump in large but non-migratory clusters. Interaction with stromal cells causes cancer cells to fragment from these static clusters into smaller, but more invasive clusters, leading to the escape of cancer cells from the inoculum.

Our results suggest that the presence of a small number of stromal cells expressing an attractive signal for migrating cancer cells can lead to a population-level increase in the ability of cancer cells to migrate long distances, and that cell clusters of significant size leaving the initial tumor site will likely be aided in their migration by stromal cells. In realistic settings, increasing the coherence of migrating cancer cell clusters may increase the aggressiveness of cancer invasion by preserving other deleterious collective phenotypes, such as pooling of paracrine growth signals or matrix-remodeling proteases [22, 48, 48, 70, 96, 140, 166]. Thus, the effect of tumor-stromal interaction to increase the number of cells that are able to migrate coherently and maintain

cell-cell signaling may increase the fitness of the invading cancer cell population [39, 80, 108].

It is now well established that collective migration can emerge within cancer even without the presence of stromal cells. This phenomenon seems to be suitably described by the 1-species SPP model [150, 149]. Here we add one degree of complexity by investigating the effect of a minority of attracting cells within on a large population. While this work is inspired by reports showing that carcinoma cells are attracted to EGF secreted by tumor-associated macrophages (Wyckoff et al. 2004), it necessarily presents a simplified view. There are potentially many other interaction processes existing within macrophages, tumor cells and their complex microenvironment [39, 108, 126]. Such interactions represent further levels of complexity that are out of the scope of this study.

Nonetheless, our simple model already shows a dramatic effect on the behavior of the population. Specifically, the emergence of system-level increases in migration distance in our Cancer-Stromal Model does not require a structured environment featuring system-level signals such as chemoattractant or extracellular matrix gradients [6]. We show that increased migration efficiency and escape of tumor cells from a primary tumor mass can be achieved purely through local, pairwise cell-cell interactions; no global migration trigger or directional cue is necessary. When we investigate the spatial distribution of stromal cells in migrating cell clusters, we find that it becomes asymmetrical and correlated with the mean polarization of the stromal cells when tumor-stromal interaction was switched on (Fig. 3.7B). This effect decreased with increasing noise (Fig. 3.7), suggesting that tumor-stromal interaction causes the stromal cells to emerge as leaders on the leading edge of their moving clusters. Still, on a the-

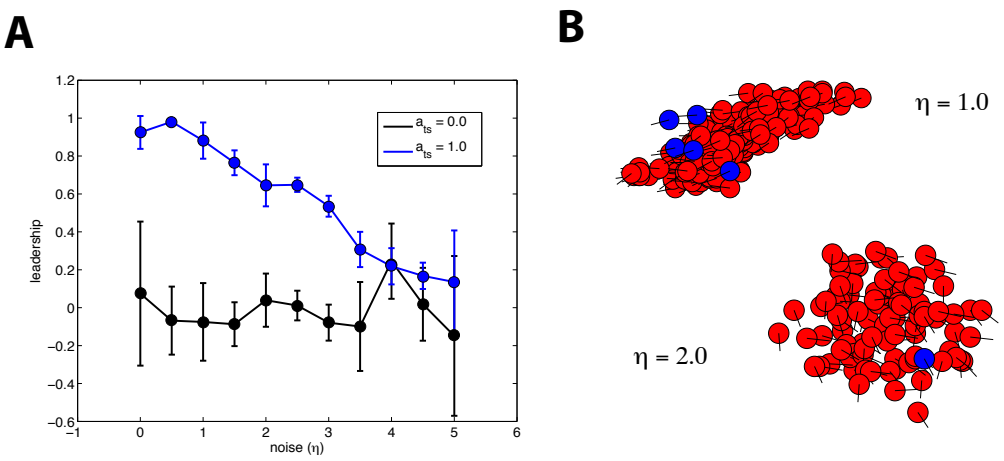

Figure 3.7: A) We defined a leadership metric as *leadership* $\equiv v_1 \cdot v_2$, where v_1 is defined as a unit vector pointing from the center of mass of a moving cell cluster to the center of mass of all stromal cells in that cluster, and v_2 is defined as the mean polarization of all stromal cells in that cluster. The leadership metric thus ranges from 1 to -1, where 1 represents the case that the stromal cells tend to be at the leading edge of cell clusters and leading them, and -1 represents the case that the stromal cells tend to be at the trailing edge of cell clusters and breaking away. We found that changing a_{ts} from 0 to 1 caused the system-wide leadership to increase, indicating the sorting of stromal cells to the front of clusters, and that this effect decayed with increasing noise. B) Representative examples of moving heterogeneous clusters from $a_{ts} = 1$ simulations.

oretical level, our model is distinct from collective migration models where the population is divided into 'leaders that are sensitive to a global directional signal (e.g. a patchy nutrient environment), and 'followers that are not [83], since in our case the stromal cells do not follow a global directional cue. On a biological level, the dynamic construction of leadership we use in the Cancer-Stromal Model reflects the experimental observation that leadership in collective cancer cell migration can be defined not by genotype but by the spatial structure of the cell population itself and differential access to microenvironmental factors [65].

It is also worth noting that our cancer-stromal model makes the assumption that long-range signaling between tumor cells and stromal cells has a digital response, vanishing at distances greater than the range of tumor-stromal inter-

action r_{ts}. To determine whether our results are an artifact of this model assumption, we performed additional simulations using a function in which the strength of the tumor-stromal interactions decayed continuously away from the stromal cell as $\frac{r_{ij}}{r_{ts}}$ with a maximum value of a_{ts}. We found that at $\eta = 1, a_{ts} = 1$, cancer cells moved toward the center of mass of the stromal cells, which, given the uniform distribution of cells at inoculation, was calculated to be the center of the simulation space. This effect is a modeling artifact due to boundary conditions used in simulations and has no relevance to biological reality. When we started decreasing $a_{ts} \rightarrow 0.01$ the artifact vanished and the simulation yielded similar results to those using Equation 3.1. Given that the two methods yielded similar results, and that the continuous interaction function increased both the degrees of freedom in the model and the computation time required, we concluded that Equation 3.1 was preferable for modeling tumor-stromal interactions. In addition, within the dense and heterogeneous tissue of real solid tumors, continuous decay over long distances may not accurately describe the distribution of diffusible molecular signals.

Recent studies on interactions between the tumor and its stromal microenvironment have generated interest in targeting the microenvironment for treatment, i.e. 'ecological therapy [79]. Our results suggest that cell-cell communication among the migrating cancer cell population may serve to amplify and increase the robustness of pro-invasive tumor-stromal interactions, propagating signals beyond the leading edge of cancer cells in direct contact with stromal cells. It may thus be necessary to consider the reinforcement of pro-tumor tumor-stromal interactions by signaling within the tumor cell population when designing and testing potential ecological therapies. A hybrid therapy targeting tumor-stromal and tumor-tumor intercellular signaling simultaneously may be

required for effectiveness.

It is worth noting that the metrics we used to quantify the performance of collective migration may be applicable to both simulated and experimental cell systems such as *in vitro* cell tracking assays [150]. By collecting phenomenological data with sufficient resolution to track the positions and velocities of individual cells and quantifying collective migration experimentally for a specific biological system (here meaning a stromal cell type and a cancer cell type), one may parameterize or 'tune a phenomenological model to reproduce the collective-level behavior of an experimental system. Such hybrid experimental/computational studies have been performed in animal [107] and cellular [150] systems. The tuned computational model may then be modified and interrogated to make testable hypotheses for the specified system; for example, to predict the co-migration patterns of cancer cells and tumor-associated macrophages in a highly structured *in vivo* environment using data collected in an unstructured *in vitro* co-culture assay, such as a chemotaxis chamber or collagen gel. We hope that our expanded SPP model will help bridge the knowledge gap between the tractability of low-perturbation *in vitro* experiments and the complexity of stromal-assisted cancer cell invasion *in vivo*.

CHAPTER 4

WITHDRAWAL OF THE PRO-TUMORAL PHENOTYPE IN TUMOR-ASSOCIATED MACROPHAGES IS SUFFICIENT FOR EFFECTIVE TREATMENT OF PLATELET-DERIVED GROWTH FACTOR-DRIVEN GLIOBLASTOMA IN MICE

This chapter has been submitted as [30] and was in review at the time of writing.

4.1 Abstract

Understanding how to disrupt protumoral interactions between tumor cells and their stromal microenvironment is crucial for the effective treatment of cancer. Because of the often complex and reciprocal nature of signaling between tumor cells and non-cancerous stromal cells, molecular therapies targeting stromal cells may result in unexpected outcomes. We dissect the dynamics of tumor growth and response to therapy by developing a mathematical model of tumor-stromal interaction dynamics. Using our model, we reveal that the outcome of treatment targeted at reeducating stromal cells away from a protumoral phenotype is dependent on the composition and size of the tumor at treatment initiation, as well as the rate of reeducating protumoral stromal cells, and the antitumoral capacity of the resultant reeducated cells. We apply our model to existing data from *in vivo* treatment of PDGF-driven glioma in a mouse model with the small molecule BLZ945 targeting colony-stimulating factor 1 (CSF-1) signaling in tumor-associated macrophages (TAMs). We conclude that the observed efficacy of treatment is largely dependent on the reeducation of protumoral TAMs and the depletion of circulating macrophage progenitors. Importantly, the antitumoral activity of TAMs reeducated by BLZ945 is only significant when it is

stronger the protumoral effect of the untreated TAMs residing in the same tumor. Our model provides a general description model of tumor growth and treatment dynamics under complex interaction with the stroma and can be extended to predict long-term efficacy and outcomes of combinatorial treatments.

4.2 Introduction

Recent research has contributed to the appreciation of cancer as a disease not only of tumor cells, but of the ecological system comprised of interactions between different tumor cell species, and between tumor cells and their microenvironment [101]. The understanding of tumors as ecosystems has generated the concept of ecological therapy: targeted treatments intended not to directly destroy malignant cancer cells, an approach which selects for drug resistance [112], but to disrupt intercellular or cell-microenvironment interactions that enable invasive growth of tumor cells or the evolutionary selection for increasingly aggressive tumor cell clones. The aim of such treatments can be to create conditions that discourage the malignant expansion of the tumor cell populations [101], reduce the selective advantage of aggressively-proliferating cells [112], or to restore homeostasis in the diseased tissues [14].

Stromal cells such as macrophages and fibroblasts are crucial components of the tumor microenvironment. Mutualistic relationships between cancer cells and stromal cells play important roles in cancer progression. For example, cancer-associated fibroblasts enable invasion [70] and angiogenesis [124], and certain tumor-associated immune cells participate in protumoral inflammation, driving growth [135], while endothelial cells and pericytes are necessary par-

ticipants in angiogenesis [20]. Significantly, amongst the myriad cells of the cancer stroma, it has been shown that tumor-associated macrophages (TAMs) are important in promoting the growth and malignancy of many solid cancers, including breast [37] and glioma [100, 133]. Alternatively activated TAMs, called M2 macrophages, are commonly considered to be anti-inflammatory and protumoral, and have been linked to the functions of macrophages in wound healing and regeneration, including matrix remodeling, growth factor secretion, immunosuppression, and angiogenesis [100]. Conversely, classically activated (M1) macrophages are considered to be anti-tumoral and pro-inflammatory [109, 120, 134]. Due to their important role in cancer proliferation, the TAM population presents an attractive target for therapy [24].

Tumor-derived CSF-1, as well as lactate [25, 35], and factors such as IL-4, IL-10, and TGF-β [100] play important roles in regulating the activation state of TAMs. In addition, in breast cancer, tumor cell-derived CSF-1 and TAM-derived EGF form a signaling feedback loop that may be important for the maintenance of TAMs in the alternatively activated state [37]. Therapeutic inhibition of the CSF-1 receptor (CSF-1R) with the small molecule PLX3397 in conjunction with chemotherapy was shown to lead to effective reduction of breast tumors in mouse models [50]. In certain contexts, CSF-1R inhibition as a monotherapy has also shown efficacy. Recently, administration of a small molecule inhibitor of CSF-1R, BLZ945, alone led to regression of PDGF-B-driven gliomas in mice [133], with the efficacy being more pronounced for tumors that were larger at the time of treatment initiation (Fig. 4.1A-D). Macrophages are depleted by dosing with BLZ945 *in vitro*; however, in *in vivo* murine PDGF-B-driven gliomas (PDG), factors secreted by tumor cells including GM-CSF and IFN-γ rescue macrophages from cell death, and treatment efficacy is associated

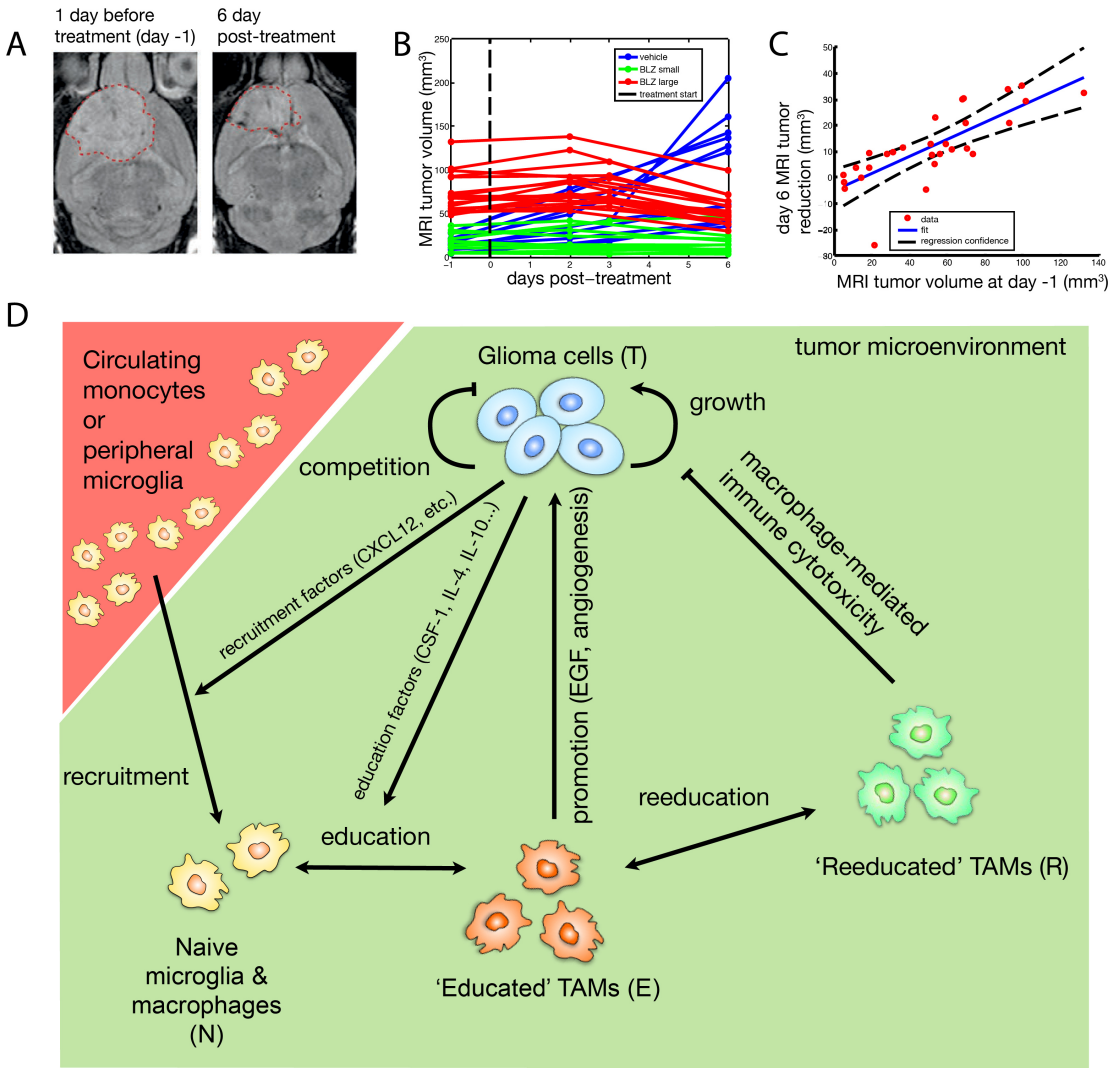

Figure 4.1: The CSF-1 receptor (CSF-1R) inhibitor BLZ945 targets the tumor microenvironment and reduces PDGF-B-driven gliomas in a mouse model. (A) Representative MRI of tumor volume decrease in a BLZ945-treated mouse. (B) TAM-targeted CSF-1R inhibition treatment of glioblastoma using BLZ945 reduces tumor volume over one week. (C) Large tumors exhibit greater reduction in size under BLZ945 treatment. (D) Diagram of cell-cell interactions in tumor population dynamics. Data presented in A-C reproduced with permission from [133]

and repolarization of TAMs away from a protumoral phenotype correlated with increased phagocytic capacity, termed TAM *reeducation* [133].

Despite this efficacy, it is currently unknown which factors contribute to

BLZ945 dependent tumor regression in murine PDGs. In addition to inhibiting macrophage dependent tumor cell proliferation *in vitro*, CSF-1R inhibition leads to decreased vascular density *in vivo* [133]. Thus, it is possible that withdrawal of educated TAMs and their support of a protumoral microenvironment, in particular the tumor vasculature, suffices to explain the effectiveness of CSF-1R inhibitor treatment. While BLZ945-treated TAMs also display increased phagocytosis of dead and dying tumor cells [133], it is unknown whether phagocytosis by treated TAMs drives the striking depletion of tumor cells in the glioma model. In addition, it is unclear if BLZ945 efficacy depends upon cytotoxic activity of TAMs, either through direct tumor cell killing by TAMs themselves or by engaging the adaptive immune system.

Here we investigate the mechanism of action of BLZ495 treatment by developing and analyzing a general mathematical model of the dynamics of tumor development and the action of tumor stroma-targeting drugs. Our model describes the dynamics of and interactions between cell subpopulations in a solid tumor in which protumoral stromal cells play a supportive role, and the alterations of these interactions under targeted therapy. We find that predicting the outcomes of ecological therapy is nontrivial, and that the efficacy of BLZ945 in PDG tumors is likely due to a combination of loss of the educated TAM phenotype and antitumoral cytotoxicity of reeducated TAMs, though the former alone may suffice for effective treatment.

4.3 Mathematical model and assumptions

We construct a mathematical population dynamics model using ordinary differential equations to describe the progression and treatment of TAM-dependent tumors using macrophage-targeted therapy. The model has four state variables, each representing a cell population: Tumor cells (T), nave macrophages (N), educated macrophages (E) and reeducated macrophages (R) (Fig. 4.1D). The model is built on four assumptions:

Assumption 1

Tumor is initiated with 1 tumor cell and no other cellular species ($T = 1, N = E = R = 0$), and tumor growth is self-limiting without stromal cells. We assume that tumor cells (T) initially proliferate independent of macrophages with coefficient μ. Proliferation is inhibited and glioma cells are driven to quiescence or death through competition for limited microenvironmental resources as they increase in density with coefficient c, resulting in self-limiting logistic growth [19]. The coefficients μ and c define the basal carrying capacity $\kappa = \frac{\mu}{c}$, the maximum size to which a tumor can grow through cell-autonomous processes.

Assumption 2

The presence of tumor cells triggers recruitment of nave macrophages or microglia (N) from either the peripheral brain, in the case of glioma, and/or the systemic circulation [133, 10, 7]. We model the rate of recruitment as a function of the tumor cell population size using a Hill function. Use of the Hill func-

tion allows us to define a critical tumor cell population size T_{crit}. In a tumor much smaller than this critical size, the rate of macrophage recruitment will be negligible, and in a much larger tumor, recruitment will be saturated; i.e. the rate of macrophage recruitment will be invariant with change in tumor size and equal to the maximum rate of recruitment, r_{max}. The steepness of this transition is determined by the Hill parameter h.

Assumption 3

Recruited macrophages are educated by interaction with tumor cells into a protumoral TAM phenotype, whose presence relaxes microenvironmental constraints on tumor cell growth. Upon infiltration of the tumor microenvironment, nave macrophages are educated through paracrine interaction with tumor cells into a protumoral TAM phenotype (E) [162]. These educated macrophages promote the growth of tumor cells, for example, through microenvironmental remodeling, immunosuppression, and promotion of angiogenesis [162, 76, 105]. Thus, the presence of educated TAMs in the tumor microenvironment effectively raises the carrying capacity of tumor cells above the basal carrying capacity $\kappa = \frac{\mu}{c}$. In effect, this renders our model a relative of established dynamic carrying capacity models for cancer growth [19, 136], but with the dynamics of the carrying capacity increase being modulated by the cell population dynamics instead of explicitly described.

Assumption 4

TAM-targeted treatment changes the rate parameters governing interactions between cell populations. We assume that TAM-targeted drugs have an on-or-off effect, and do not introduce new processes to the network of intercellular signals, but modify the rates of existing interactions and of switching between TAM phenotypes. To this end, we introduce five parameters of varying value that determine the effect of treatment on interactions between cellular subpopulations. Reeducated neutral or anti-tumoral TAMs (R) induce cytotoxicity against tumor cells determined by the parameter α. The drug inhibits the protumoral signaling of educated TAMs by a fraction β; for example, this could represent the effect of inhibitors that negate angiogenic signals produced by educated TAMs. The rate of nave macrophage education is modulated by the coefficient γ. The rate of reeducation of educated TAMs is modulated by the coefficient δ. Finally, the rate of recruitment of macrophages and microglia is reduced by a fraction ϵ. The values of these parameters are only used when drug is present in the tumor; for untreated or vehicle-treated tumors, they default to the values of $\beta = 0, \gamma = 1, \delta = 1, \epsilon = 0$. α retains its set value regardless of drug presence. By including the possibility of multiple alterations to the intercellular signaling network, we account for the variation in dynamics of anti-TAM therapy between different tumors.

Figure 4.1E shows a diagram of tumor-macrophage interactions and the parameters affected by treatment in our model. The full set of differential equa-

tions constituting the model is as follows:

$$\frac{dT}{dt} = \mu T - cT^2 + g(1-\beta)E - \alpha RT \tag{4.1}$$

$$\frac{dN}{dt} = r_{max}\frac{1}{1+(T_{crit}/T)^h} - \gamma k_1 NT + k_2 E \tag{4.2}$$

$$\frac{dE}{dt} = \gamma k_1 NT - k_2 E - \delta k_3 E + k_4 R \tag{4.3}$$

$$\frac{dR}{dt} = \delta k_3 E - k_4 R \tag{4.4}$$

Table 4.1 lists the model parameters and their definitions. Calculations for estimating fixed-value parameters are described in the Methods section.

We performed numerical simulations of the model and analyzed the equations to predict the long-term tumor size, composition, and growth rate. We make further simplifying assumptions about the model dynamics to obtain the latter analytical solutions.

4.4 Rationale of parameter values

4.4.1 Estimation of tumor cell population size from MRI data

Vehicle-treated tumors have typical volumes of $10 - 100\text{mm}^3$, as measured by MRI. Approximating cells as cubes $\approx 10\mu$m on a side (BNID 108941, [114]), a typical eukaryotic cell has a volume of 10^{-6}mm^3. Hence, we estimate a tumor of volume order 10mm^3 to contain on the order of 10^7 cells, and a tumor of volume order 100mm^3 to contain 10^8 cells.

Parameter	Definition	Dimensions (ND = non-dimensional)	Values used	Rationale
μ	tumor cell growth rate constant	Tumor cell/time	0.7 cells/day	See 4.4.2
c	tumor cell competition rate constant	1/(tumor cell * time)	7×10^{-8} day	See 4.4.3
g	coefficient of promotion by educated TAMs	1/(stromal cell * time)	6.3×10^{-7} /(stromal cell * day)	See 4.4.4
r_{max}	max rate of recruitment of stromal cells	Stromal cell/time	10^6 stromal cells/day	See 4.4.5
T_{crit}	critical tumor cell population size for recruitment of stromal cells	Tumor cell	10^7 cells	See 4.4.6
h	Hill constant of recruitment rate function	ND	2	See 4.4.6
k_1	rate constant of education of naïve stromal cells to a pro-tumoral phenotype	1/time	1000	See 4.4.6
k_2	rate constant of reversion of educated stromal cells to the naïve phenotype	1/time	0	See 4.4.6
k_3	rate constant of reeducation of educated stromal cells to a neutral or anti-tumoral phenotype	1/time	0.001	See 4.4.6
k_4	rate constant of reversion of reeducated stromal cells to the educated phenotype	1/time	1	See 4.4.6
α	cytotoxicity induced by reeducated stromal cells	1/(stromal cell * time)	$[10^{-9}, 10^{-3}]$ /(stromal cell * time)	See 4.4.6
β	fractional inhibition of pro-tumoral signaling from educated stromal cells by treatment	ND	$[0, 1]$	See 4.4.6
γ	modulation of educated rate by treatment	ND	$[0.001, 1]$	See 4.4.6
δ	modulation of reeducation rate by treatment	ND	$[1, 10^4]$	See 4.4.6
ϵ	fractional inhibition of stromal cell recruitment by treatment	ND	$[0, 1]$	See 4.4.6

Table 4.1: Parameters used in the tumor-macrophage population dynamics model

4.4.2 Estimation of tumor cell growth constant

Assuming a population of T cells undergoing exponential growth, the effective growth coefficient μ can be calculated from the population doubling time τ:

$$T(\tau) = T(0)e^{\mu\tau} \tag{4.5}$$

$$\frac{T(\tau)}{T(0)} = 2 = e^{\mu\tau} \tag{4.6}$$

$$\mu = \frac{\ln 2}{e} \tag{4.7}$$

4.4.3 Estimation of tumor cell competition constant

Linear regression of tumor reduction as a function of initial tumor size predicts tumors of size approximately 20mm^3 will not be reduced by BLZ945 treatment. Assuming that the majority of cells in the tumor are tumor cells, and that this volume is equal to the basal (logistic) carrying capacity of the tumor cells, which is a function of the tumor cell growth and competition constants $\kappa = 20\text{mm}^3 \approx 10^7\text{cells} = \frac{\mu}{c}$, therefore

$$c = 7 \times 10^{-8}(\text{cells} \times \text{day})^{-1} \tag{4.8}$$

4.4.4 Estimation of educated TAM promotion constant

Experiments show TAMs to constitute roughly 10% of all cells in vehicle-treated gliomas. Assuming this composition is steady-state,

$$f_{mac}^{*} = \frac{c}{c+g} = 0.1 \tag{4.9}$$

Therefore,

$$g = 6.3 \times 10^{-7} (\text{TAMs} \times \text{day})^{-1} \tag{4.10}$$

4.4.5 Estimation of max macrophage/microglia recruitment rate

The long-term growth rate of vehicle-treated tumors is predicted to be

$$\left(\frac{dT}{dt}\right)^{*} = \frac{g r_{max} f_E}{c} \tag{4.11}$$

Estimating from MRI measurements, the growth rate of vehicle-treated tumors during the final week of experiment is constant and approximately $\left(\frac{dT}{dt}\right)^{*} = 10^7$ cells/day. Assuming all TAMs in untreated tumors are educated ($f_E \approx 1$), we estimate

$$r_{max} = 10^6 \text{ macrophages/day} \tag{4.12}$$

4.4.6 Other parameters

T_{crit}

Simulations with various values of T_{crit} as a function of $\kappa = \frac{\mu}{c}$ were performed (see 4.6.1). Though variations in $\frac{T_{crit}}{\kappa}$ produced noticeable variations in the early growth stage of simulated untreated tumors, the long-term dynamics were identical. From the data in [133], the value of $\frac{T_{crit}}{\kappa}$ cannot be determined. We thus used $T_{crit} = \kappa$ for simplicity in subsequent simulations.

h

We used a Hill function with exponent 2 to model a nonlinear transition in the dynamics of monocyte recruitment from negligible at low glioma cell count to saturated at high glioma cell counts. An upper limit for monocyte influx is reasonable, given that the circulating/peripheral monocyte population and tumor blood vessel density are finite. Saturation dynamics in the form of Michaelis-Menten functions have conventionally been used to model the dynamics of immune cell recruitment [47], identical to a Hill function with exponent 1. Using an exponent of 2 additionally models weak recruitment of monocytes at low glioma cell count. This can be interpreted as tumor inflammation, which correlates with immune cell infiltration and malignancy, being triggered only when the glioma cell population size and cellular stress become significant [108].

k_i

Without time-resolved imaging of expression of polarization marker genes in macrophages, it is difficult to set biologically accurate values for the rate constants of macrophage phenotypic transitions. Values were chosen such that almost all TAMs in untreated tumors would be educated (i.e. $\frac{E}{N+E+R} \approx 1$). The actual relative abundance of educated TAMs *in vivo* may differ. Results from [133] suggest several differentially-regulated genes associated with the M2 polarization of macrophages that could be useful as an *in vivo* marker for macrophages expressing the educated phenotype, including Arg1 and Mrc1. However, though increased expression of these genes on the population level correlates with increased tumor growth, macrophage polarization occurs along a spectrum, and it is possible not all macrophages expressing these genes have a protumoral educated phenotype. More rigorous methods of categorizing macrophage phenotypes with respect to their phenomenological impact on the growth of glioma cells is required to accurately determine these parameters.

Setting $k_i \ll \mu, c, g$ could possibly lead to macrophage polarization dynamics lagging the bulk tumor cell and macrophage population dynamics, and consequently generate oscillatory behavior. However, this would require the time scale of macrophage intracellular regulatory signaling be far longer than the time scale of cellular apoptosis and macrophage infiltration. Without further knowledge of the dynamics of regulatory networks governing macrophage polarization, this possibility seems unlikely to be realistic.

$\alpha, \beta, \gamma, \delta, \epsilon$

The five parameters governing the dynamics of TAM reeducation treatment represent phenomenological values of putative alterations to cell-cell interactions. We performed a thorough parameter scan of each parameter (between 0 and 1 for parameters representing relative inhibitions in rate, where 0 is full inhibition and 1 is no inhibition; across orders of magnitude for parameter representing absolute values). Parameter values were further fixed for the specific case of BLZ945 treatment of glioma (see 4.6.3).

4.5 Methods

A system of ordinary differential equations (eqs. 4.1-4.4) was implemented in the Matlab programming language. The equations were solved numerically using the integration routine *ode15s*.

4.6 Results and discussion

4.6.1 Simulations of untreated tumors

Analysis of the model reveals that in tumors that depend on educated TAMs for progression, tumor growth occurs in compositionally distinct stages. Initially, when the tumor size is small, macrophage recruitment is negligible and growth is limited by the intrinsic growth rate of cancer cells. At $T \approx T_{crit}$, macrophage recruitment accelerates until the rate of recruitment stabilizes to

r_{max}. As a result, the macrophage content of the tumor increases rapidly. The recruited macrophages are educated by interactions with tumor cells and display the protumoral TAM phenotype, increasing the rate of glioma cell proliferation and rescuing tumor growth from self-limitation due to previous microenvironmental scarcity.

As a result, tumor growth occurs in three compositionally distinct phases: an initial phase of macrophage-poor, glioma cell-autonomous growth, followed by a transient phase of accelerating TAM enrichment and growth, and finally a linear growth phase in which glioma cells and macrophages rapidly increase in number while remaining in constant proportion (Fig 4.2). Assuming all macrophages in the tumor are reeducated TAMs, the steady-state fraction of TAMs in untreated gliomas (f^*_{mac}) can be predicted as a function of the glioma cell competition coefficient c and the educated TAM promotion coefficient g:

$$f^*_{mac} = \left(\frac{T}{T+M}\right) = \frac{c}{c+g} \tag{4.13}$$

Given the above solution for the projected TAM content of a tumor, and assuming the equilibrium between naïve and educated TAMs is rapidly reached, the rate of malignant glioma growth in the long-term $\left(\frac{dT}{dt}\right)^*$ is a function of the promotion coefficient, the maximum rate of macrophage recruitment r_{max}, and the competition coefficient:

$$\left(\frac{dT}{dt}\right)^* = \frac{g r_{max} f_E}{c} \tag{4.14}$$

Notably, the final linear phase of tumor growth is faster than early, macrophage-free growth. This corroborates experimental observations that macrophage infiltration precedes the onset of angiogenesis and malignancy *in vivo* [25].

The specific dynamics of the transition from initial low-macrophage growth to malignant macrophage-dependent growth depends on whether the basal car-

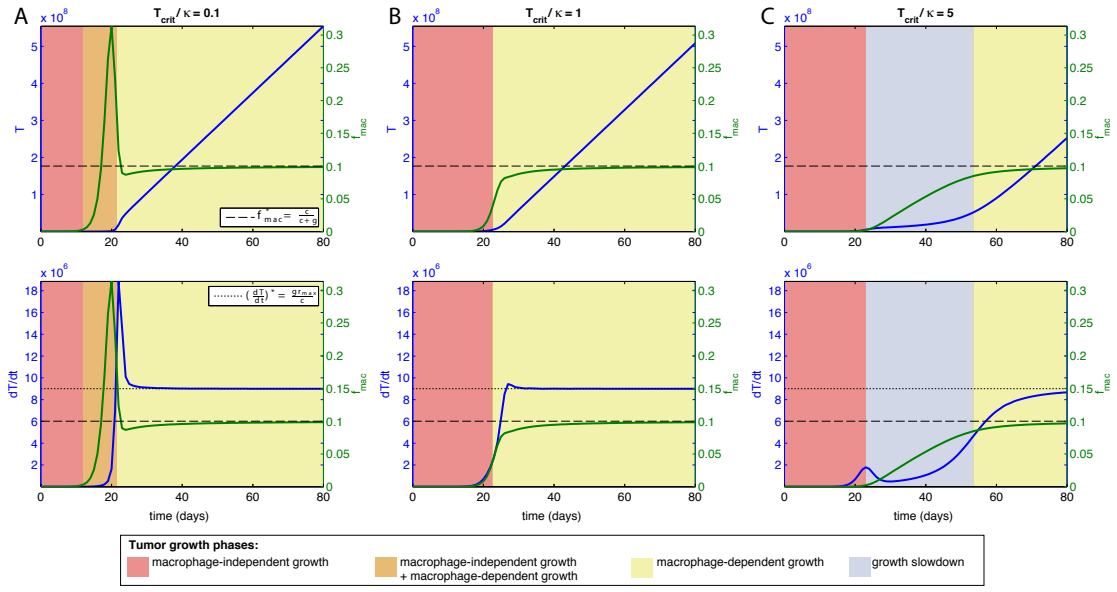

Figure 4.2: Effects of varying $\frac{T_{crit}}{\kappa}$ on tumor growth dynamics. Left axes, top row: tumor cell count as a function of time. Left axes, bottom row: tumor cell growth rate as a function of time. Right axes: relative macrophage abundance as a function of time. (A) $\frac{T_{crit}}{\kappa} < 1$ generates an initial slow phase of TAM-independent growth of constant rate, followed by a fast phase of concurrent TAM-dependent and TAM-independent growth, and finally a slower phase of TAM-dependent growth only of constant rate. (B) $\frac{T_{crit}}{\kappa} = 1$ generates an initial slow phase of TAM-independent growth of constant rate followed by a smooth acceleration to TAM-dependent only growth of constant rate, with no overlap between the two phases. (C) $\frac{T_{crit}}{\kappa} > 1$ generates an initial slow phase of TAM-independent growth of constant rate, followed by an exponential TAM-independent growth and quiescence, followed by TAM-dependent growth of saturating rate.

rying capacity of the glioma cells is reached before the transition from slow to rapid macrophage recruitment, that is the ratio of parameters $\frac{T_{crit}}{\kappa}$. When $\frac{T_{crit}}{\kappa} \leq 1$, rapid macrophage recruitment begins before the basal carrying capacity is reached: this leads to a transient phase when TAM-independent growth and TAM-dependent growth proceed simultaneously, resulting in very fast growth until the basal carrying capacity is reached, after which the tumor size increases more slowly and only through TAM-dependent growth (Fig. 4.2A). When $\frac{T_{crit}}{\kappa} = 1$, the tumor progresses via TAM-independent growth until reach-

ing the basal carrying capacity, followed immediately by a transition to TAM-dependent growth (Fig. 4.2B). When $\frac{T_{crit}}{\kappa} \geq 1$, the tumor progresses via TAM-independent growth until reaching the basal carrying capacity, followed by a period of apparent tumor dormancy. However, during this quiescent phase, the tumor continues to recruit and educate macrophages, thus enabling growth at a lower rate. Once the glioma cell population size reaches T_{crit}, macrophage recruitment accelerates, and the tumor enters the final phase of fast, malignant growth (Fig. 4.2C). Our model thus reveals multistage compositional dynamics in early glioma growth that may be difficult to detect *in vivo*.

Interestingly, in the case of $\frac{T_{crit}}{\kappa} = 1$, the dynamics generated by our model resemble those of the established exponential-linear model featuring two distinct growth phases separated by a threshold tumor mass, which has been shown to describe accurately the growth of ovarian and colorectal [145] and breast [19] xenograft tumors in mouse models. Our model thus reveals a possible cancer ecological explanation for previously observed bulk tumor growth dynamics that may apply to solid tumors in different tissues.

4.6.2 Simulations of treated tumors

We first developed a generalized model of tumor treatment based on targeting the macrophage compartment of stromal cells. Although this model was motivated by the success of BLZ945 glioma treatment in glioma models, the model presented here also allows investigation of other treatments that target TAMs. We assume that the properties of any TAM-targeted therapy fall within a five-dimensional parameter space $(\alpha, \beta, \gamma, \delta, \epsilon)$. After performing a parameter scan of

this space (Table 1), we find that qualitative treatment outcomes fall into one of four categories:

1. reduced and suppressed (regression)

2. reduced, but not suppressed (tumor rebounds after reaching a minimum size: relapse)

3. not reduced, but suppressed (stasis)

4. not reduced, and not suppressed, with tumor progression continuing at a slowed rate (progressive disease) (Fig. 4.3).

The model also predicts that the tumor cell population under continuous treatment will achieve a minimum size before becoming suppressed or before rebound occurs. For purposes of analysis, we assume that TAM reeducation is effectively instantaneous, all macrophages in the tumor adopt either the educated TAM or the reeducated TAM phenotype, and that tumor reduction under treatment occurs before any recruitment of nave macrophages into the tumor. Under these assumptions, the reduction in tumor size achieved before relapse or suppression is a function of the relative abundances of educated and reeducated TAMs, the basal carrying capacity of tumor cells, as well as the tumor cell population size at the time of treatment initiation.

$$\Delta T = T(t_d)\left[1 - \left((1-\beta)\, f_E^* - \frac{\alpha}{g} f_R^*\right)\right] - \kappa \tag{4.15}$$

Where $T_(t_d)$ is the number of tumor cells at the time of treatment initiation, and f_E^*, f_R^* are the post-treatment steady-state solutions for the relative abundances

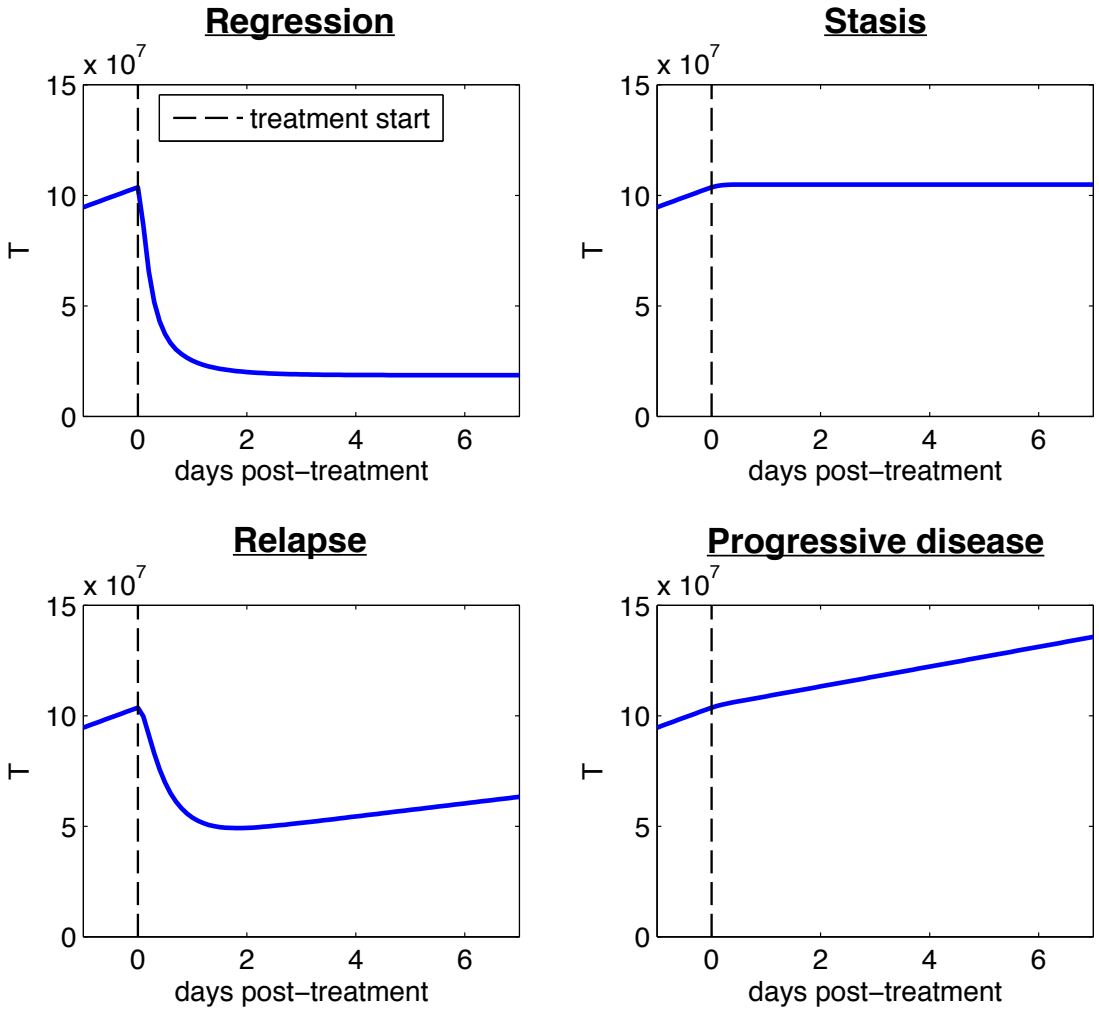

Figure 4.3: Qualitative categories of TAM-targeted treatment outcomes. Transient tumor reduction efficacy does not guarantee effective long-term suppression of tumor progression, as illustrated by the panel "relapse".

of educated TAMs and reeducated TAMs. These relative abundances are determined from the treatment parameter δ and the equilibrium ratio of reeducated to educated TAMs K_r, which can be calculated from the rate constants of TAM

reeducation and reversion to the educated phenotype:

$$K_r = \frac{k_3}{k_4} \tag{4.16}$$

$$f_E^* = \frac{1}{1 + \delta K_r} \tag{4.17}$$

$$f_R^* = \frac{\delta K_r}{1 + \delta K_r} \tag{4.18}$$

Assuming the parameters governing intercellular interactions are consistent between pre-treatment tumors, this translates into a positive linear relationship between the total number of cells in the tumor at time of treatment initiation and residual tumor size after treatment. This replicates the linear correlation between pre- and post-treatment tumor size seen in *in vivo* experiments with the PDG model (Fig. 4.1C). It is also evident that any reduction of the tumor beneath the basal carrying capacity ($T_{min} < \kappa$) requires the reeducated TAMs to possess antitumoral cytotoxicity greater than the ratio of the post-treatment promotional coefficient $g(1 - \beta)$ to the post-treatment reeducated to educated TAM ratio δK_r:

$$\alpha > \frac{g(1 - \beta)}{\delta K_r} \tag{4.19}$$

Similarly to the pre-treatment case, we can solve the equations to obtain the long-term change in tumor cell carrying capacity under continuous treatment, which will determine whether tumor rebound occurs. The rate of change in tumor cell carrying capacity is equal to the rate of change of the steady-state solution for the tumor cell population size:

$$\frac{dT^*}{dt} = \frac{dM}{dt}\frac{1}{c}(g(1 - \beta)f_E^* - \alpha f_R^*) \tag{4.20}$$

Assuming macrophage recruitment is the only source of fluctuations in the total number of macrophages in the tumor, that is, all other processes such as

macrophage cell death and in situ proliferation sum to zero:

$$\frac{dM}{dt} = (1-\epsilon) r_{max} \frac{1}{1+(T_{crit}/T)^h} \tag{4.21}$$

From this solution it is evident that tumor growth will be successfully suppressed by continuous treatment if at least one of the following conditions is met:

1. The tumor cell population is reduced to a small enough size, such that $\frac{1}{1+(T_{crit}/T)^h} \approx 0$;

2. Recruitment of nave macrophages is effectively blocked, i.e. $\epsilon = 1$;

3. The cytotoxic effect of reeducated macrophages is high enough such that $\alpha > \frac{g(1-\beta)}{\delta K_r}$.

Either of the first two conditions ensures further macrophage recruitment will be inhibited, preventing TAM-dependent tumor relapse, while the third condition means any continued macrophage recruitment will have an overall antitumoral effect due to treatment-induced macrophage reeducation. On the contrary, if none of these conditions are met, the tumor may rebound under continuous treatment, despite initially effective tumor reduction. Our model thus reveals a mechanism for the non-evolutionary emergence of resistance to anti-TAM therapy under continuous treatment, enabled purely by population dynamics.

4.6.3 Applying the model to explain BLZ945 mechanism of action in glioma mouse models

We then apply our generalized mathematical model to the specific case of BLZ945 treatment of PDGF-driven glioblastoma in mice. The following experimental observations [133] allow us to constrain the model of untreated tumor growth:

- Magnetic resonance imaging (MRI) of vehicle-treated mice shows linear expansion of tumor volume within a seven-day observation period post-treatment initiation (Fig. 4.1A)

- linear regression of fractional tumor reduction as a function of tumor size at time of treatment, as measured by MRI, predicts that tumors smaller than $\approx$ 20mm^3 will initially continue to grow during BLZ945 treatment, slowing and eventually arresting as T approaches κ (Fig. 4.1C).

- immunostaining and flow cytometry of vehicle-treated tumors show relative TAM abundance of 10-20% [133].

The precise dynamics of early tumor growth in PDGF-driven glioma are unknown and may differ from other TAM-rich solid tumors. Our model predicts that the value of T_{crit} has no impact on the long-term tumor growth rate, which makes it is difficult to estimate the value from *in vivo* MRI measurements. These data represent later TAM-rich stages of glioma growth.

In addition to this, empirical values for T_{crit} and κ may represent glioma cell counts smaller than the MRI detection threshold and thus are below the detection limit. Research has shown that myeloid infiltration into murine gliomas is largely dependent upon HIF-1α signaling and subsequent CXCL12 mediated recruitment [55]. Further studies have shown a similar mechanism at play in response to irradiation therapy [99]. We infer from these studies that cellular stresses experienced during early gliomagenesis and conventional therapy are indicative of the stresses that a tumor experiences as it reaches its basal carrying capacity, interpretable as the maximum allowable tumor size without macrophages. Thus, we assume that the rate of macrophage recruitment increases dramatically as $T \rightarrow \kappa$. In other words, we assume that the critical tumor size equals the tumor intrinsic carrying capacity: $T_{crit} = \kappa$.

In preclinical experiments, BLZ945 treatment is initiated when a tumor of detectable size is observed via MRI, usually around week 5 post-tumor initiation; mice are thereafter dosed daily with drug [133]. We thus assume that BLZ945 enters and remains in the system at a constant level after treatment initiation. When BLZ945 is present, educated TAMs are converted to the reeducated phenotype. We simulate tumor growth by initializing simulations (day 0) with 1 glioma cell and no other cellular species present. As in the experiments, we fix the time of treatment initiation at $t_{drug} = 35$ days. Simulations were run for 42 days.

From *in vivo* experiments, it is known that circulating monocytes and brain-resident microglia, the presumed precursors of TAMs, are depleted by BLZ945, eliminating the reservoir of macrophages that may be recruited to the tumor to expand the carrying capacity [133]. We thus assume that macrophage recruit-

ment post-BLZ945 treatment is completely inhibited, or $\epsilon = 1$. From our solution to the generic model above, this is sufficient to explain the lack of tumor rebound observed in the experimental system (Fig. 4.3).

The initial education of naïve macrophages into a protumoral phenotype and inhibition of the antitumoral phenotype is likely to be driven by a complex set of signals not limited to CSF-1, including CCL2 [169], GM-CSF [144], IL-4, IL-10, and IL-13 [76, 110]. We thus assume that the education of naïve macrophages is not inhibited by BLZ945, and therefore $\gamma = 1$.

Finally, if any TAMs remain in the educated compartment, it can be assumed that the ability of glioma cells to benefit from their presence is not altered by BLZ945, thus we set $\beta = 0$ [133].

Therefore, after considering the constraints imposed by experimental observations, the five-dimensional parameter space of the generic treatment model is reduced to a two-dimensional subspace (α, δ), for the specific case of BLZ945 treatment of PDGF-driven glioblastoma. In other words, the efficacy of the treatment is dependent only upon the anti-glioma cell cytotoxicity induced by the reeducated TAMs (α) and the rate of TAM reeducation (δ). We performed a parameter scan of the two-dimensional phase space across seven orders of magnitude of α and five orders of magnitude of δ and found two distinct regions of behavior separated by the line $\alpha = \frac{g}{\delta K_r}$ (Fig. 4.4). In the lower region, the tumor is not completely eliminated, even though further progression is suppressed. The efficiency of the regression is mainly a function of the reeducation (parameter δ). In the upper region, the tumor cell population is completely eliminated by BLZ945 treatment. The influence of α on the outcome of treatment largely disappears with values $< 10^{-7}$, meaning the cytotoxicity induced

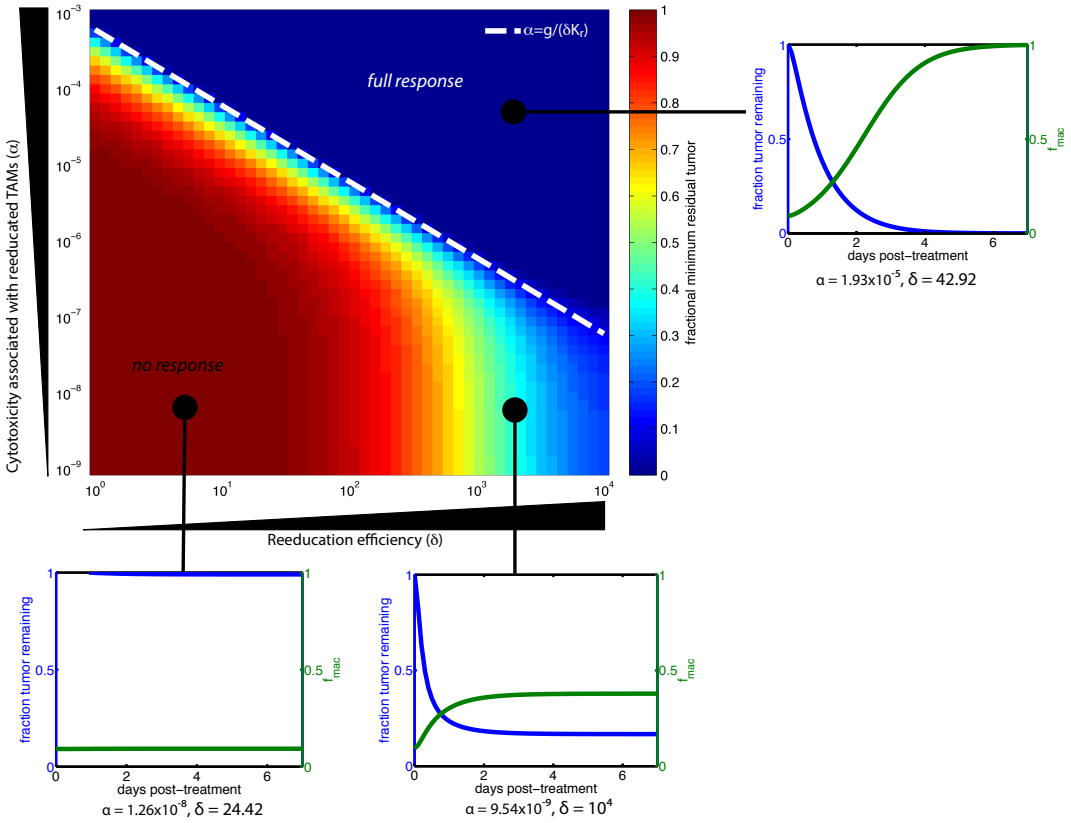

Figure 4.4: Minimum residual tumor size relative to the tumor size at time of treatment initiation in the phase space of (δ, α). White dotted line indicates the separation between the upper-right domain where the tumor cells are completely depleted, and the lower-left domain where they are not, and represents the critical reeducated TAM cytotoxicity relative to rate of reeducation $\alpha = \frac{g}{\delta K_r}$. When $\alpha < 10^{-7} = g$ reeducated TAM cytotoxicity has a negligible effect on treatment outcome, and efficacy is determined solely by the rate of reeducation. Insets: representative time courses.

by reeducated TAMs is weaker than the protumoral effect of educated TAMs, and the loss of educated TAMs and the consequent withdrawal of a protumoral stromal microenvironment are responsible for generating the bulk of treatment efficacy. With $\alpha > 10^{-7)}$, meaning the cytotoxicity induced by reeducated TAMs is stronger than the protumoral effect of educated TAMs, antitumoral cytotoxicity in reeducated TAMs becomes a significant factor in treatment outcome.

4.7 Discussion

Ecological interactions amongst cancer cells and between cancer cells and the stroma drive the population responses of tumors to physiological challenges during progression and treatment, leading to malignancy and drug resistance [123]. Quantitative understanding of cancer ecology will be crucial to the development of successful therapeutic strategies, and effective categorization of disease based on recognition of population-level ecological 'biomarkers such as tumor composition and intratumoral heterogeneity. Mathematical modeling can be a powerful tool to describe and predict the dynamics of disease progression and treatment.

Pro-tumoral signaling from stromal cells such as TAMs (but also including, for example, cancer-associated fibroblasts [142]) perform essential functions in tumor progression. Our model shows the growth of such a tumor, composed of a heterogenous and mutualistically-interacting population of tumor and stromal cells, and exhibits complex population dynamics and fluctuations of population composition. Similarly, the post-treatment dynamics of the cellular populations show that outcomes can be nonlinear and vary over time, as well as depend on the state of the tumor at time of treatment initiation. Our results raise the possibility that the assessment of treatment efficacy for general stromal-targeted therapies is thus complicated even without considering the emergence of resistance through evolutionary mechanisms, and may require differentiating between short-term tumor regression and long-term tumor suppression.

Owing to factors such as tumor-associated inflammation [57] and the fragility of tumor vasculature [46, 115], the tumor microenvironment is highly

heterogeneous and unstable [59, 69, 71, 155]. Such an unstable microenvironment may require constant remodeling to maintain its pro-tumoral properties. TAMs expressing an alternatively activated, regenerative phenotype may play important roles in maintenance of a pro-tumoral microenvironment [81, 134, 141]. In treating a tumor system dependent on TAMs for microenvironmental maintenance with TAM reeducation factors, it may not be necessary to induce expression of an anti-tumoral macrophage phenotype to successfully regress the tumor. However, anti-tumoral killing by reeducated TAMs can suppress tumor regrowth in cases where residual macrophage recruitment and educated TAMs persist.

Specific to the activity of BLZ945 in the glioma model, we find induction of anti-tumoral cytotoxicity in the re-educated TAMs not to be required for the effectiveness of treatment seen in *in vivo* experiments [133]. Indeed, our model predicts that when anti-tumoral cytotoxicity mediated by re-educated TAMs is weaker than pro-tumoral signaling in educated TAMs, this anti-tumoral activity will have negligible impact on treatment outcome (Fig. 4.4). However, this cytotoxicity-independent efficacy is dependent on the inhibition of macrophage recruitment, possibly due to the depletion of circulating monocytes, and alternative CSF-1R inhibitors or TAM-targeted agents that do not deplete circulating monocytes or inhibit their recruitment may have different outcomes. Furthermore, variations between tumors, or between tumors of different types, mean that some tumor cell populations may receive a greater beneficial effect from educated TAMs, i.e. g is greater. For these tumors, we predict with our model that reeducated TAMs must induce greater cytotoxicity for TAM-targeted ecological therapy to be effective, assuming the efficiency of re-education is the same.

The complexity of tumor-TAM signaling provides many possible mechanisms for intervention by treatment, and our general model provides a means to predict the therapeutic efficacy of those interventions. For example, the effect of inhibiting signals from pro-tumoral stromal cells, such as microglia-derived IL-6 in glioma [169], without depleting or altering the phenotypes of the stromal cells, may be modeled by setting the parameter $\beta > 0$. The action of anti-angiogenic factors such as anti-VEGF inhibitors [75] could be similarly modeled. Interestingly, the (δ, α) phase space of BLZ945 treatment shows that the domains of full response and no response are separated by a relatively narrow boundary, implying that for some tumors with limited or no response, a small change in parameters could generate a large change in response, possibly leading to full regression of the tumor. This suggests a role for combinatorial treatments. For example, BLZ945 combined with a hypothetical treatment increasing the anti-tumoral immune activity associated with reeducated TAMs (α) by 10-fold could drive a partially responsive or non-responsive tumor to full response. For this reason, TAM reeducation could serve as a powerful complement or alternative to treatments aimed at depleting or preventing the recruitment of macrophages [23].

We acknowledge that our model does not capture the full complexity of tumor-stromal ecology and perturbations to it. Current analyses do not investigate the response of tumor ecology to conventional treatments, such as radiotherapy and chemotherapy, which rapidly deplete tumor cells but do not target stromal cells. Modeling the response of the tumor-stromal system to a sudden decrease in tumor cell count could be implemented in a future application of our model. We also have not modeled the protective effect of tumor cell-secreted factors on TAMs in the face of CSF-1R inhibition, which specifi-

cally prevented TAM killing, while microglia and other normal macrophages were depleted [133]. Conceivably, loss of tumor cells upon initial TAM reeducation followed by TAM loss due to depletion of those protective tumor cells could result in a feedback that would suffice for effective treatment. Finally, it would be interesting to investigate the possibility of dynamic regulation of multiple independent pro-tumoral signaling pathways within educated TAMs, such as IGF-1 [68], as each macrophage phenotypic compartment is modeled as internally homogeneous and invariant with time. In sum, we present a general mathematical model to predict the outcomes of tumor growth and treatment with respect to the complex interactions between tumor cells and associated stromal cells, as well as alterations in their respective phenotypes after targeted therapy. We have used our model to examine possible factors explaining the efficacy of BLZ945 treatment of PDGF-driven glioma in a mouse model [133]. The model may be expanded to predict longer-term outcomes of continued treatment, including relapse after discontinuation of treatment, or loss of treatment effectiveness through emergence of resistance.

CHAPTER 5

CONCLUSIONS

5.1 The importance of being collective

In light of increased capability for characterizing tumors in terms of genomic alteration and gene expression on a per-patient basis, there has been anticipation that the next paradigm shift in cancer treatment will come in the form of *personalized medicine* [102]. Under this paradigm, the disease of each cancer patient would be categorized into a subtype based on identification of genomic and transcriptomic biomarkers, after which the most effective course of treatment for that subtype would be applied.

Despite the promise of personalized treatment, inter- and intra-tumoral heterogeneity present several possible obstacles to its success [61]:

- The initial number of qualified recipients of personalized therapy might be small, as driving genetic alterations are difficult to identify in many cancers, attributable to phenotypic complexity and genomic instability of transformed cells [56];

- while sophisticated and specific treatments may be highly effective, the number of cases in which they are useful may be limited, as driving genomic events that recur across cancer types are rare [3];

- due to intratumoral clonal heterogeneity, targeted treatments are unlikely

to affect all cells in the tumor, leading to high risk of relapse driven by non-responsive clones.

In short, there is a threat that perceived tumor complexity will explosively increase with diagnostic resolution, resulting in the disintegration of cancer into a plethora of individual complex diseases for which costly treatments must be designed respectively, to a point that the impact of any novel targeted treatment on the overall long-term cancer risk of the patient population becomes negligible and not worth the investment necessary to develop it. In anticipation of this explosion of complexity, it is now essential to understand not only how tumors are different, but how they are the same: to focus on discovering first principles governing the behavior of tumors as intricate multicellular systems that are generalizable across patients and cancer types despite underlying heterogeneity at the cellular and molecular levels.

Without understanding these principles, the qualitative large-scale and long-term outcomes of molecular events cannot be accurately predicted, and findings cannot be transferred between mechanistically diverse systems. Because of this, phenomenological models, such as those I have described here, inferred from and validated against data will form a necessary complement to mechanistic models and experiments. For while a mechanistic view of cancer may identify therapeutic targets, phenomenology describes the effects of perturbations of mechanism on the flow of information through the system. Thus, phenomenological models can provide the means of predicting the observed evolution of a system from its observed initial state.

Existing efforts to study complex systems such as cancer cell populations and cellular signaling networks often take a hypothesis- and modeling-driven

approach. Indeed, the two projects presented in this dissertation fall under this category. Such approaches risk obscuring not only the true complexity and magnitude of biological populations or signaling networks, but perhaps more importantly, the characteristic ability of real biological systems to produce relevant behaviors on multiple time- and length-scales [104]. The emerging challenge is to learn the organizing principles of complex biological networks and populations directly from data, including large-scale genomic and transcriptomic data, which is now becoming increasingly available [12]. In closing, I will outline several proposals for experimentally probing the ecological and evolutionary complexity of cancer in ways that can also yield meaningful theoretical insight.

5.2 Proposed experimental approaches to cancer ecology and evolution

5.2.1 From 'big data'

Intratumoral cellular heterogeneity in solid tumors on the genomic [74, 168] and phenotypic [130] levels has been observed using sequencing techniques. Although such datasets can reveal the cellular composition of tumors, an extra layer of analysis is necessary to infer the population structure—that is, the topology of interactions between cellular subpopulations that generate and sustain the expansionary population dynamics that characterize malignancy.

One promising course of research would be to infer quantitative, phenomenological models of interactions between cell subpopulations in cancers

from sequencing data. Inspiration for this approach can be found in recent studies of the human gut microbiome [148, 60]. In these works, time series of the abundances of bacterial species (more accurately operational taxonomic units, or OTUs) in human digestive systems are obtained by sequencing microbial DNA, then quantifying the abundance of each bacterial species through qPCR amplification of distinguishing 16S ribosomal RNA. Coefficients for Lotka-Volterra population dynamics models are then inferred from time series species abundances using various techniques.

Within the population of transformed cells, genome sequencing will be useful in reconstructing the phylogenetic tree of transformed clones [51]. The major challenge in applying this methodology to cancer is that much of intratumoral phenotypic heterogeneity is driven by microenvironmental regulation and the plasticity of intracellular signaling networks. Hence, distinctive genomic variations between functional cellular subpopulations in tumors are likely to be rare. All untransformed stromal and infiltrating immune cells, in particular, will be genomically identical with each other and with all other untransformed cells of the host. It thus becomes necessary to characterize cells phenotypically on the level of gene expression, if not function.

A distribution of cells in gene expression space can be obtained through single-cell transcriptome profiling [43], and categorized into transcriptional subtypes using machine learning methods such as unsupervised clustering. Alternatively, bulk tumor transcriptome data could be decomposed along mean gene expression patterns of different cell types to reconstruct the abundances of cellular subpopulations. An example of decomposition of expression data along expression patterns characteristic cell types exists for identifying putative can-

cer stem cells in acute myeloid leukemia [72]. Time-resolved data of this kind would allow the inference of a dynamical model of interactions between subpopulations from the time correlation of their abundances.

As time series data may be difficult to obtain in a clinical environment, an alternative approach could be to search for correlations between phenotypic subpopulations across samples of different tumors, or samples from different spatial locations within the same tumor. As correlation between variables in a network does not imply a direct interaction, a stepwise regression method such as that used in [60] could be used to weed out indirect interactions from the putative ecological network.

A parallel path could be to discover predictive population-level disease markers within the network of intercellular interactions. Currently recognized clinical markers such as tumor morphology and genetic signatures neglect the role of the cellular ecosystem in determining the outcomes of cancer progression and treatment [50, 98]. By inferring the underlying networks of interactions between cellular populations in cancer and analyzing their topologies, it could analyze the robustness of tumors to microenvironmental challenges and therapies, and identify weak points in the ecological interaction network which, when perturbed with treatment, might drive the collapse or growth arrest of the cancer cell population. Such weak points may involve, for example, positive feedback interactions between cancer cells and protumoral stromal cells.

In addition, it is possible that the mapping of cancer cellular composition to multicellular phenotype is degenerate, allowing tumors with disparate cellular compositions to exhibit similar large-scale and long-term behavior. If this degeneracy is found to be relevant to cancer, this could reduce the functional

complexity of intertumoral heterogeneity, and explain non-cell autonomous resistance of cancer to treatments that deplete or inhibit the activity of certain cell subpopulations.

5.2.2 From *in vivo* experiment

Novel experimental methods such as intravital microscopy have allowed for the direct imaging of fluorescent-tagged cell subpopulations in solid tumors [2]. Using such techniques, experimentalists have been able to observe the *in vivo* emergence of collective cancer cell streaming as a result of pro-invasive feedback signaling between breast cancer cells and tumor-associated macrophages through the EGF/CSF-1 paracrine loop [140]. However, such experiments require keeping the host animal in a stressed and weakened state, and may not be feasible for more long-term observations.

For shorter time scale phenomena such as collective motion, spinning disk confocal microscopy can provide real-time live-animal imaging of single cells [58, 32]. From such videos, correlation functions can be calculated for cell clusters engaged in collective migration. This would open the path to a quantitative and phenomenological model of information transfer between moving cells. Such a study would be analogous to animal studies [28, 8, 107] where phenomenological interactions governing collective motion have been inferred from high-resolution videos of moving groups. Fluorescence correlation spectroscopy measurements of the same collective migration events could corroborate phenomenological interactions with molecular mechanisms by recording the formation and aggregation of E-cadherin complexes [153], through which

biochemical and mechanical signals are communicated between collectively migrating cells.

Longer time scale population-dynamical experiments could be performed using conventional mouse model techniques. A recent study [111] observes clonal interference in a mouse xenograft system. Cell lines of a common genetic background were divided into sub-lineages each over-expressing a single secreted factor, mixed, and transplanted into mice. In perhaps their most striking result, a subclone over-expressing interlelukin 11 proved capable of driving the expansion of the bulk tumor while decreasing in frequency, exhibiting what is defined evolutionarily as altruistic behavior. Studies in fruit flies also observed tumorigenesis driven by clonal cooperation [163, 121].

The weakness of these existing studies is they rely on synthetic generation of a panel of cellular subpopulations. Hence, the phenotypic heterogeneity observed is a result of artificial manipulations and not the native selective pressures and noise experienced by cells residing in a nascent tumor in living tissue. Thus, even when one observes interesting cell population dynamics and tumor growth patterns resembling those of clinical tumors, these may not prove an accurate reproduction of either the small-scale mechanisms or the long-term bulk dynamics of clinical tumors. Indeed, the long-term population dynamics of [163] and [111] both result in the extinction of the tumor-driving clone, and presumably the arrest of tumor progression, at which point the salient question then becomes: how does a tumor exploit either evolution or phenotypic plasticity to adapt when it, e.g., exhausts a source of key cytokines?

For this reason, a more ideal approach may be to initiate tumors natively using transgenic techniques, or an (ostensibly) clonal xenograft inoculum, then

observe the development and evolution of the cell population over time. For such an approach, a useful platform may be the transparent *casper* zebrafish model [159]. This model allows non-invasive imaging of fluorescent-tagged cells as they proliferate and migrate through the host animal. Combined with a Cre-based lineage tracing technique (a.k.a. 'zebrabow') [129], this would enable descendent lineages of a clonal xenograft inoculum to be tracked through the full timescale of disease progression. Using this method, it may be possible to infer Lotka-Volterra population dynamics models of differentially-labeled subclones at primary and metastatic sites.

5.2.3 From *in vitro* experiment

Ecological and evolutionary experiments have been performed over long timescales in microbial populations [154, 161]. Such experiments show potential for translating to *in vitro* co-culture experiments using cancer cell lines and possibly stromal cell lines. The problem is that the collective response observed would be stripped of the context of the selective pressures of the *in vivo* tumor microenvironment. Over longer time scales, the discrepancy in culture conditions could have an increasing impact on the relevance of observations. A biomimetic culture platform could approximate *in vivo* microenvironmental conditions [92], but in general more large-scale evolutionary experiments should probably be left for *in vivo* settings.

On the other hand, *in vitro* studies could be useful in probing the emergent dynamics of specific signaling pathways of interest in collectives of cells. As evidenced in modeling-driven collective motion studies, simple stimuli-

response mechanisms may nonetheless produce interesting behavior when integrated across an interconnected network of individuals differentially affected by spatial positioning and thermodynamic fluctuation. Culture experiments have yielded results observing collective motion of cells in chick keratocytes sufficient for parameterizing an SPP model [150]. The SPP model of collective motion can be regarded as a 1- to 3-dimensional analogue of the Ising model of ferromagnetism [156]. That is, the 1- to 3-dimensional velocity vector of each moving individual aligns and becomes correlated with that of other individuals as a function of their spatial positions and velocities. For experimental systems of interaction cells in motion, an interaction matrix can be inferred from the velocity correlations.

This approach can perhaps be further generalized to correlations between n-dimensional gene expression vectors of individual cells in culture, where for experiments that will be both relevant and tractable, n is constrained at the lower bound by the number of relevant signaling molecules in a given paracrine-coupled regulatory pathway, and at the upper bound by the number of signaling molecules that may be quantified in real-time with multichannel fluorescent labeling. An elemental example of such an experiment may be found in the studies of Gregor *et al.* [143] on cyclic AMP signaling in the social amoeba *Dictystelium*. Here, the correlated variable is a 1-dimensional vector consisting of the cytosolic cAMP concentration of each cell.

BIBLIOGRAPHY

[1] C Athena Aktipis and Randolph M Nesse. Evolutionary foundations for cancer biology. *Evol Appl*, 6(1):144–159, January 2013.

[2] Stephanie Alexander, Bettina Weigelin, Frank Winkler, and Peter Friedl. Preclinical intravital microscopy of the tumour-stroma interface: invasion, metastasis, and therapy response. *Current Opinion in Cell Biology*, 25(5):659–671, October 2013.

[3] Laufey T Amundadottir, Sverrir Thorvaldsson, Daniel F Gudbjartsson, Patrick Sulem, Kristleifur Kristjansson, Sigurdur Arnason, Jeffrey R Gulcher, Johannes Bjornsson, Augustine Kong, Unnur Thorsteinsdottir, and Kari Stefansson. Cancer as a complex phenotype: Pattern of cancer distribution within and beyond the nuclear family. *PLoS Med*, 1(3):e65, December 2004.

[4] Alexander R. A. Anderson. A hybrid mathematical model of solid tumour invasion: the importance of cell adhesion. *Mathematical medicine and biology : a journal of the IMA*, 22(2):163–86, June 2005.

[5] Alexander R. A. Anderson and Vito Quaranta. Integrative mathematical oncology. *Nature reviews. Cancer*, 8(3):227–34, March 2008.

[6] Alexander R. A. Anderson, Alissa M. Weaver, Peter T. Cummings, and Vito Quaranta. Tumor morphology and phenotypic evolution driven by selective pressure from the microenvironment. *Cell*, 127(5):905–915, December 2006.

[7] Lisa M. Arendt, Jessica McCready, Patricia J. Keller, Dana D. Baker, Stephen P. Naber, Victoria Seewaldt, and Charlotte Kuperwasser. Obesity promotes breast cancer by CCL2-mediated macrophage recruitment and angiogenesis. *Cancer Res*, 73(19):6080–6093, October 2013.

[8] A. Attanasi, A. Cavagna, L. Del Castello, I. Giardina, S. Melillo, L. Parisi, O. Pohl, B. Rossaro, E. Shen, E. Silvestri, and M. Viale. Collective behaviour without collective order in wild swarms of midges. *arXiv:1307.5631 [cond-mat, physics:physics, q-bio]*, July 2013.

[9] Robert Axelrod, David E Axelrod, and Kenneth J Pienta. Evolution of cooperation among tumor cells. *PNAS*, 103(36):13474–9, September 2006.

[10] Behnam Badie and Jill M. Schartner. Flow cytometric characterization of tumor-associated macrophages in experimental gliomas. *Neurosurgery April 2000*, 46(4):957–962, 2000.

[11] Linge Bai, Manolya Eyiyurekli, Peter I. Lelkes, and David E. Breen. Self-organized sorting of heterotypic agents via a chemotaxis paradigm. *Science of Computer Programming*, October 2012.

[12] Albert-László Barabási. The network takeover. *Nature Physics*, 8(1):14–16, January 2012.

[13] D Basanta, J G Scott, M N Fishman, G Ayala, S W Hayward, and A R A Anderson. Investigating prostate cancer tumour-stroma interactions: clinical and biological insights from an evolutionary game. *Br. J. Cancer*, 106(1):174–181, January 2012.

[14] David Basanta and Alexander R. A. Anderson. Exploiting ecological principles to better understand cancer progression and treatment. *Interface Focus*, 3(4), August 2013.

[15] Lazaros Batsilas, Alexander M. Berezhkovskii, and Stanislav Y. Shvartsman. Stochastic model of autocrine and paracrine signals in cell culture assays. *Biophysical Journal*, 85(6):3659–3665, December 2003.

[16] R. Bellman, H. Kagiwada, and R. Kalaba. Inverse problems in ecology. *J. Theor. Biol.*, 11(1):164–167, May 1966.

[17] Julio Belmonte, Gilberto Thomas, Leonardo Brunnet, Rita de Almeida, and Hugues Chaté. Self-propelled particle model for cell-sorting phenomena. *Physical Review Letters*, 100(24):20–23, June 2008.

[18] Eshel Ben-Jacob, Inon Cohen, and Herbert Levine. Cooperative self-organization of microorganisms. In *Advances in Physics*, volume 49, pages 395–554. June 2000.

[19] Sébastien Benzekry, Clare Lamont, Afshin Beheshti, Amanda Tracz, John M. L. Ebos, Lynn Hlatky, and Philip Hahnfeldt. Classical mathematical models for description and prediction of experimental tumor growth. *PLoS Comput Biol*, 10(8):e1003800, August 2014.

[20] Gabriele Bergers, Steven Song, N. Meyer-Morse, Emily Bergsland, and Douglas Hanahan. Benefits of targeting both pericytes and endothelial

cells in the tumor vasculature with kinase inhibitors. *Journal of Clinical Investigation*, 111(9):1287–1296, 2003.

[21] Neil A Bhowmick, Anna Chytil, David Plieth, Agnieszka E Gorska, Nancy Dumont, Scott Shappell, M Kay Washington, Eric G Neilson, and Harold L Moses. TGF-beta signaling in fibroblasts modulates the oncogenic potential of adjacent epithelia. *Science (New York, N.Y.)*, 303(5659):848–51, February 2004.

[22] François-Clément Bidard, Jean-Yves Pierga, Anne Vincent-Salomon, and Marie-France Poupon. A "class action" against the microenvironment: do cancer cells cooperate in metastasis? *Cancer metastasis reviews*, 27(1):5–10, March 2008.

[23] Laura Bonapace, Marie-May Coissieux, Jeffrey Wyckoff, Kirsten D. Mertz, Zsuzsanna Varga, Tobias Junt, and Mohamed Bentires-Alj. Cessation of CCL2 inhibition accelerates breast cancer metastasis by promoting angiogenesis. *Nature*, advance online publication, October 2014.

[24] Robert L Bowman and Johanna A Joyce. Therapeutic targeting of tumor-associated macrophages and microglia in glioblastoma. *Immunotherapy*, 6(6):663–666, June 2014.

[25] C Carmona-Fontaine, V Bucci, L Akkari, M Deforet, JA Joyce, and JB Xavier. Emergence of spatial structure in the tumor microenvironment due to the warburg effect. *Proceedings of the National Academy of Sciences*, 10(48):19402–19407, 2013.

[26] Carlos Carmona-Fontaine, Helen K Matthews, Sei Kuriyama, Mauricio Moreno, Graham a Dunn, Maddy Parsons, Claudio D Stern, and Roberto Mayor. Contact inhibition of locomotion in vivo controls neural crest directional migration. *Nature*, 456(7224):957–61, December 2008.

[27] Carlos Carmona-Fontaine, Eric Theveneau, Apostolia Tzekou, Masazumi Tada, Mae Woods, Karen M. Page, Maddy Parsons, John D. Lambris, and Roberto Mayor. Complement fragment c3a controls mutual cell attraction during collective cell migration. *Dev. Cell*, 21(6):1026–1037, December 2011.

[28] Andrea Cavagna, Alessio Cimarelli, Irene Giardina, Giorgio Parisi, Raffaele Santagati, Fabio Stefanini, and Massimiliano Viale. Scale-free correlations in starling flocks. *Proceedings of the National Academy of Sciences of the United States of America*, June 2010.

[29] W. K. Chang, C. Carmona-Fontaine, and J. B. Xavier. Tumour-stromal interactions generate emergent persistence in collective cancer cell migration. *Interface Focus*, 3(4):20130017–20130017, June 2013.

[30] William K Chang, Robert L. Bowman, Johanna A. Joyce, and João B. Xavier. Ecological therapy of cancer: withdrawal of the protumoral phenotype in tumor-associated macrophages is sufficient for effective treatment. *Submitted*.

[31] William K Chang, William C Wimley, Peter C Searson, Kalina Hristova, and Mikhail Merzlyakov. Characterization of antimicrobial peptide activity by electrochemical impedance spectroscopy. *Biochimica et biophysica acta*, 1778(10):2430–6, October 2008.

[32] Kevin J. Cheung, Edward Gabrielson, Zena Werb, and Andrew J. Ewald. Collective invasion in breast cancer requires a conserved basal epithelial program. *Cell*, 155(7):1639–1651, December 2013.

[33] Seok Chung, Ryo Sudo, Vernella Vickerman, Ioannis K. Zervantonakis, and Roger D. Kamm. Microfluidic platforms for studies of angiogenesis, cell migration, and cell–cell interactions. *Ann Biomed Eng*, 38(3):1164–1177, March 2010.

[34] Gilles Clermont and Sven Zenker. The inverse problem in mathematical biology. *Mathematical Biosciences*, October 2014.

[35] Oscar R. Colegio, Ngoc-Quynh Chu, Alison L. Szabo, Thach Chu, Anne Marie Rhebergen, Vikram Jairam, Nika Cyrus, Carolyn E. Brokowski, Stephanie C. Eisenbarth, Gillian M. Phillips, Gary W. Cline, Andrew J. Phillips, and Ruslan Medzhitov. Functional polarization of tumour-associated macrophages by tumour-derived lactic acid. *Nature*, advance online publication, July 2014.

[36] V. P. Collins, R. K. Loeffler, and H. Tivey. Observations on growth rates of human tumors. *Am J Roentgenol Radium Ther Nucl Med*, 76(5):988–1000, November 1956.

[37] John Condeelis and Jeffrey W Pollard. Macrophages: obligate partners for tumor cell migration, invasion, and metastasis. *Cell*, 124(2):263–6, January 2006.

[38] John Condeelis and Jeffrey E Segall. Intravital imaging of cell movement in tumours. *Nature Reviews Cancer*, 3(12):921–30, December 2003.

[39] Lisa M Coussens and Zena Werb. Inflammation and cancer. *Nature*, 420(6917):860–7, 2002.

[40] ID Couzin and Jens Krause. Self-organization and collective behavior in vertebrates. *Advances in the Study of Behavior*, 32:1–75, 2003.

[41] Zoltan Csahok and Andras Czirok. Hydrodynamics of bacterial motion. *Physica A: Statistical and Theoretical Physics*, 243(3-4):8, November 1998.

[42] András Czirók, Eshel Ben-Jacob, Inon Cohen, and Tamás Vicsek. Formation of complex bacterial colonies via self-generated vortices. *Physical Review E*, 54(2):1791–1801, August 1996.

[43] Piero Dalerba, Tomer Kalisky, Debashis Sahoo, Pradeep S. Rajendran, Michael E. Rothenberg, Anne A. Leyrat, Sopheak Sim, Jennifer Okamoto, Darius M. Johnston, Dalong Qian, Maider Zabala, Janet Bueno, Norma F. Neff, Jianbin Wang, Andrew A. Shelton, Brendan Visser, Shigeo Hisamori, Yohei Shimono, Marc van de Wetering, Hans Clevers, Michael F. Clarke, and Stephen R. Quake. Single-cell dissection of transcriptional heterogeneity in human colon tumors. *Nat Biotech*, 29(12):1120–1127, December 2011.

[44] Anusuya Das, Douglas Lauffenburger, Harry Asada, and Roger D Kamm. A hybrid continuum-discrete modelling approach to predict and control angiogenesis: analysis of combinatorial growth factor and matrix effects on vessel-sprouting morphology. *Philosophical transactions. Series A, Mathematical, physical, and engineering sciences*, 368(1921):2937–60, June 2010.

[45] Daniel J Dauer, Bernadette Ferraro, Lanxi Song, Bin Yu, Linda Mora, Ralf Buettner, Steve Enkemann, Richard Jove, and Eric B Haura. Stat3 regulates genes common to both wound healing and cancer. *Oncogene*, 24(21):3397–408, May 2005.

[46] Katrien De Bock, Sandra Cauwenberghs, and Peter Carmeliet. Vessel abnormalization: another hallmark of cancer?: Molecular mechanisms and therapeutic implications. *Current Opinion in Genetics & Development*, 21(1):73–79, February 2011.

[47] Lisette G de Pillis, Ami E Radunskaya, and Charles L Wiseman. A validated mathematical model of cell-mediated immune response to tumor growth. *Cancer research*, 65(17):7950–8, September 2005.

[48] Thomas S Deisboeck and Iain D Couzin. Collective behavior in cancer cell populations. *BioEssays : news and reviews in molecular, cellular and developmental biology*, 31(2):190–7, February 2009.

[49] George D. Demetri, Margaret von Mehren, Charles D. Blanke, Annick D. Van den Abbeele, Burton Eisenberg, Peter J. Roberts, Michael C. Heinrich, David A. Tuveson, Samuel Singer, Milos Janicek, Jonathan A. Fletcher, Stuart G. Silverman, Sandra L. Silberman, Renaud Capdeville, Beate Kiese, Bin Peng, Sasa Dimitrijevic, Brian J. Druker, Christopher Corless, Christopher D.M. Fletcher, and Heikki Joensuu. Efficacy and safety of imatinib mesylate in advanced gastrointestinal stromal tumors. *New England Journal of Medicine*, 347(7):472–480, August 2002.

[50] David G. DeNardo, Donal J. Brennan, Elton Rexhepaj, Brian Ruffell, Stephen L. Shiao, Stephen F. Madden, William M. Gallagher, Nikhil Wadhwani, Scott D. Keil, Sharfaa A. Junaid, Hope S. Rugo, E. Shelley Hwang, Karin Jirström, Brian L. West, and Lisa M. Coussens. Leukocyte complexity predicts breast cancer survival and functionally regulates response to chemotherapy. *Cancer Discovery*, 1(1):54–67, June 2011.

[51] Amit G. Deshwar, Shankar Vembu, Christina K. Yung, Gun Ho Jang, Lincoln Stein, and Quaid Morris. Reconstructing subclonal composition and evolution from whole genome sequencing of tumors. *arXiv:1406.7250 [cs, q-bio, stat]*, June 2014. arXiv: 1406.7250.

[52] D. Dingli, F. a. C. C. Chalub, F. C. Santos, S. Van Segbroeck, and J. M. Pacheco. Cancer phenotype as the outcome of an evolutionary game between normal and malignant cells. *Br J Cancer*, 101(7):1130–1136, September 2009.

[53] Vera S. Donnenberg and Albert D. Donnenberg. Multiple drug resistance in cancer revisited: The cancer stem cell hypothesis. *The Journal of Clinical Pharmacology*, 45(8):872–877, 2005.

[54] Alberto d'Onofrio. A general framework for modeling tumor-immune system competition and immunotherapy: Mathematical analysis and biomedical inferences. *Physica D: Nonlinear Phenomena*, 208(3-4):220–235, September 2005.

[55] Rose Du, Kan V. Lu, Claudia Petritsch, Patty Liu, Ruth Ganss, Emmanuelle Passegué, Hanqiu Song, Scott Vandenberg, Randall S. Johnson, Zena Werb, and Gabriele Bergers. HIF1alpha induces the recruitment of

bone marrow-derived vascular modulatory cells to regulate tumor angiogenesis and invasion. *Cancer Cell*, 13(3):206–220, March 2008.

[56] W. Du and O. Elemento. Cancer systems biology: embracing complexity to develop better anticancer therapeutic strategies. *Oncogene*, September 2014.

[57] H.F. Dvorak. Tumors: Wounds that do not heal. *New England Journal of Medicine*, 315(26):1650–1659, 1986.

[58] Mikala Egeblad, Elizabeth S Nakasone, and Zena Werb. Tumors as organs: complex tissues that interface with the entire organism. *Developmental cell*, 18(6):884–901, June 2010.

[59] Veronica Estrella, Tingan Chen, Mark Lloyd, Jonathan Wojtkowiak, Heather H Cornnell, Arig Ibrahim-Hashim, Kate Bailey, Yoganand Balagurunathan, Jennifer M Rothberg, Bonnie F Sloane, Joseph Johnson, Robert a Gatenby, and Robert J Gillies. Acidity generated by the tumor microenvironment drives local invasion. *Cancer research*, 73(5):1524–35, March 2013.

[60] Charles K. Fisher and Pankaj Mehta. Identifying keystone species in the human gut microbiome from metagenomic timeseries using sparse linear regression. *arXiv:1402.0511 [q-bio]*, February 2014. arXiv: 1402.0511.

[61] Rosalie Fisher, James Larkin, and Charles Swanton. Inter and intratumour heterogeneity: a barrier to individualized medical therapy in renal cell carcinoma? *Genitourinary Oncology*, page 49, 2012.

[62] Keith T. Flaherty, Igor Puzanov, Kevin B. Kim, Antoni Ribas, Grant A. McArthur, Jeffrey A. Sosman, Peter J. O'Dwyer, Richard J. Lee, Joseph F. Grippo, Keith Nolop, and Paul B. Chapman. Inhibition of mutated, activated BRAF in metastatic melanoma. *New England Journal of Medicine*, 363(9):809–819, August 2010.

[63] Jasmine Foo and Franziska Michor. Evolution of resistance to targeted anti-cancer therapies during continuous and pulsed administration strategies. *PLoS computational biology*, 5(11):e1000557, November 2009.

[64] Peter Friedl and Stephanie Alexander. Cancer invasion and the microenvironment: Plasticity and reciprocity. *Cell*, 147(5):992–1009, November 2011.

[65] Peter Friedl and Darren Gilmour. Collective cell migration in morphogenesis, regeneration and cancer. *Nature reviews. Molecular cell biology*, 10(7):445–57, July 2009.

[66] Peter Friedl, P.B. Noble, P.A. Walton, D.W. Laird, P.J. Chauvin, R.J. Tabah, Martin Black, and K.S. Zänker. Migration of coordinated cell clusters in mesenchymal and epithelial cancer explants in vitro. *Cancer research*, 55(20):4557, 1995.

[67] Peter Friedl and Katarina Wolf. Plasticity of cell migration: a multiscale tuning model. *The Journal of cell biology*, 188(1):11–9, January 2010.

[68] Jason M. Fritz, Lori D. Dwyer-Nield, and Alvin M. Malkinson. Stimulation of neoplastic mouse lung cell proliferation by alveolar macrophage-derived, insulin-like growth factor-1 can be blocked by inhibiting MEK and PI3k activation. *Mol. Cancer*, 10:76, 2011.

[69] Dai Fukumura and Rakesh K. Jain. Tumor microenvironment abnormalities: Causes, consequences, and strategies to normalize. *J. Cell. Biochem.*, 101(4):937–949, July 2007.

[70] Cedric Gaggioli, Steven Hooper, Cristina Hidalgo-Carcedo, Robert Grosse, John F Marshall, Kevin Harrington, and Erik Sahai. Fibroblast-led collective invasion of carcinoma cells with differing roles for RhoGTPases in leading and following cells. *Nature cell biology*, 9(12):1392–400, December 2007.

[71] Robert A. Gatenby, Edward T. Gawlinski, Arthur F. Gmitro, Brant Kaylor, and Robert J. Gillies. Acid-mediated tumor invasion: a multidisciplinary study. *Cancer Res*, 66(10):5216–5223, May 2006.

[72] Andrew J. Gentles, Sylvia K. Plevritis, Ravindra Majeti, and Ash A. Alizadeh. A leukemic stem cell gene expression signature is associated with clinical outcomes in acute myeloid leukemia. *JAMA*, 304(24):2706–2715, December 2010.

[73] M. Gerlinger and C. Swanton. How darwinian models inform therapeutic failure initiated by clonal heterogeneity in cancer medicine. *Br J Cancer*, 103(8):1139–1143, October 2010.

[74] Marco Gerlinger, Andrew J. Rowan, Stuart Horswell, James Larkin, David Endesfelder, Eva Gronroos, Pierre Martinez, Nicholas Matthews, Aengus

Stewart, Patrick Tarpey, Ignacio Varela, Benjamin Phillimore, Sharmin Begum, Neil Q. McDonald, Adam Butler, David Jones, Keiran Raine, Calli Latimer, Claudio R. Santos, Mahrokh Nohadani, Aron C. Eklund, Bradley Spencer-Dene, Graham Clark, Lisa Pickering, Gordon Stamp, Martin Gore, Zoltan Szallasi, Julian Downward, P. Andrew Futreal, and Charles Swanton. Intratumor heterogeneity and branched evolution revealed by multiregion sequencing. *NEJM*, 366(10):883–892, 2012.

[75] Elizabeth R. Gerstner and Tracy T. Batchelor. Antiangiogenic therapy for glioblastoma. *Cancer J*, 18(1):45–50, February 2012.

[76] Vasilena Gocheva, Hao-Wei Wang, Bedrick B Gadea, Tanaya Shree, Karen E Hunter, Alfred L Garfall, Tara Berman, and Johanna a Joyce. IL-4 induces cathepsin protease activity in tumor-associated macrophages to promote cancer growth and invasion. *Genes & development*, 24(3):241–55, February 2010.

[77] Isabel González-García, Ricard V. Solé, and José Costa. Metapopulation dynamics and spatial heterogeneity in cancer. *PNAS*, 99(20):13085–13089, October 2002.

[78] Sumanta Goswami, Erik Sahai, Jeffrey B Wyckoff, Michael Cammer, Dianne Cox, Fiona J Pixley, E Richard Stanley, Jeffrey E Segall, and John S Condeelis. Macrophages promote the invasion of breast carcinoma cells via a colony-stimulating factor-1/epidermal growth factor paracrine loop. *Cancer research*, 65(12):5278–83, June 2005.

[79] Mel Greaves and Carlo C Maley. Clonal evolution in cancer. *Nature*, 481(7381):306–13, January 2012.

[80] Sergei I Grivennikov, Florian R Greten, and Michael Karin. Immunity, inflammation, and cancer. *Cell*, 140(6):883–99, March 2010.

[81] Chunqing Guo, Annicole Buranych, Devanand Sarkar, Paul B. Fisher, and Xiang-Yang Wang. The role of tumor-associated macrophages in tumor vascularization. *Vascular Cell*, 5(1):20, December 2013.

[82] Piyush B Gupta, Christine M Fillmore, Guozhi Jiang, Sagi D Shapira, Kai Tao, Charlotte Kuperwasser, and Eric S Lander. Stochastic state transitions give rise to phenotypic equilibrium in populations of cancer cells. *Cell*, 146(4):633–44, August 2011.

[83] Vishwesha Guttal and Iain D Couzin. Leadership, collective motion and the evolution of migratory strategies. *Communicative & integrative biology*, 4(3):294–8, May 2011.

[84] Oskar Hallatschek, Pascal Hersen, Sharad Ramanathan, and David R. Nelson. Genetic drift at expanding frontiers promotes gene segregation. *arXiv*, (1), December 2008.

[85] Douglas Hanahan and Lisa M. Coussens. Accessories to the crime: Functions of cells recruited to the tumor microenvironment. *Cancer Cell*, 21(3):309–322, March 2012.

[86] Douglas Hanahan and Robert A Weinberg. The hallmarks of cancer. *Cell*, 100:57–70, 2000.

[87] Douglas Hanahan and Robert a Weinberg. Hallmarks of cancer: the next generation. *Cell*, 144(5):646–74, March 2011.

[88] Yael Hegerfeldt, Miriam Tusch, Eva-B Bröcker, and Peter Friedl. Collective cell movement in primary melanoma explants: plasticity of cell-cell interaction, beta1-integrin function, and migration strategies. *Cancer research*, 62(7):2125–30, April 2002.

[89] Gloria H. Heppner. Cancer cell societies and tumor progression. *Stem Cells*, 11(3):199–203, 1993.

[90] Patrick C. Hermann, Stephan L. Huber, Tanja Herrler, Alexandra Aicher, Joachim W. Ellwart, Markus Guba, Christiane J. Bruns, and Christopher Heeschen. Distinct populations of cancer stem cells determine tumor growth and metastatic activity in human pancreatic cancer. *Cell Stem Cell*, 1(3):313–323, September 2007.

[91] Sui Huang, Gabriel Eichler, Yaneer Bar-Yam, and Donald E. Ingber. Cell fates as high-dimensional attractor states of a complex gene regulatory network. *Physical Review Letters*, 94(12), April 2005.

[92] Dietmar W. Hutmacher. Biomaterials offer cancer research the third dimension. *Nat Mater*, 9(2):90–93, February 2010.

[93] Johanna a Joyce and Jeffrey W Pollard. Microenvironmental regulation of metastasis. *Nature reviews. Cancer*, 9(4):239–52, April 2009.

[94] Alexandre J Kabla. Collective cell migration: leadership, invasion and segregation. *Journal of the Royal Society, Interface / the Royal Society*, 9(77):3268–78, December 2012.

[95] Leo P Kadanoff. Scaling and universality in statistical physics. *Physica A: Statistical Mechanics and its Applications*, 163(1):1–14, February 1990.

[96] Dmitriy Kedrin, Bojana Gligorijevic, Jeffrey Wyckoff, Vladislav V. Verkhusha, John Condeelis, Jeffrey E. Segall, and Jacco van Rheenen. Intravital imaging of metastatic behavior through a mammary imaging window. *Nat. Methods*, 5(12):1019–1021, December 2008.

[97] Antoine a Khalil and Peter Friedl. Determinants of leader cells in collective cell migration. *Integrative biology : quantitative biosciences from nano to macro*, 2(11-12):568–74, November 2010.

[98] Seung Wook Kim, Hyun Jin Choi, Ho-Jeong Lee, Junqin He, Qiuyu Wu, Robert R. Langley, Isaiah J. Fidler, and Sun-Jin Kim. Role of the endothelin axis in astrocyte- and endothelial cell-mediated chemoprotection of cancer cells. *Neuro-oncology*, 16(12):1585–1598, December 2014.

[99] Mitomu Kioi, Hannes Vogel, Geoffrey Schultz, Robert M. Hoffman, Griffith R. Harsh, and J. Martin Brown. Inhibition of vasculogenesis, but not angiogenesis, prevents the recurrence of glioblastoma after irradiation in mice. *J. Clin. Invest.*, 120(3):694–705, March 2010.

[100] Y Komohara, K Ohnishi, J Kuratsu, and M Takeya. Possible involvement of the m2 anti-inflammatory macrophage phenotype in growth of human gliomas. *The Journal of pathology*, 216(1):15–24, September 2008.

[101] Kirill S. Korolev, Joao B. Xavier, and Jeff Gore. Turning ecology and evolution against cancer. *Nat Rev Cancer*, 14(5):371–380, May 2014.

[102] Nicholas B. La Thangue and David J. Kerr. Predictive biomarkers: a paradigm shift towards personalized cancer medicine. *Nat Rev Clin Oncol*, 8(10):587–596, October 2011.

[103] Kevin Leder, Ken Pitter, Quincey LaPlant, Dolores Hambardzumyan, Brian D. Ross, Timothy A. Chan, Eric C. Holland, and Franziska Michor. Mathematical modeling of PDGF-driven glioblastoma reveals optimized radiation dosing schedules. *Cell*, 156(3):603–616, January 2014.

[104] S. Levin. The problem of pattern and scale in ecology: The robert h. MacArthur award lecture. *Ecology*, 73(6):1943–1967, 1992.

[105] Elaine Y. Lin, Jiu-Feng Li, Leoid Gnatovskiy, Yan Deng, Liyin Zhu, Dustin A. Grzesik, Hong Qian, Xiao-nan Xue, and Jeffrey W. Pollard. Macrophages regulate the angiogenic switch in a mouse model of breast cancer. *Cancer Res*, 66(23):11238–11246, December 2006.

[106] L. A. Loeb. Mutator phenotype may be required for multistage carcinogenesis. *Cancer Res.*, 51(12):3075–3079, June 1991.

[107] Ryan Lukeman, Yue-Xian Li, and Leah Edelstein-Keshet. Inferring individual rules from collective behavior. *Proceedings of the National Academy of Sciences of the United States of America*, 107(28):12576–80, July 2010.

[108] Alberto Mantovani, Paola Allavena, Antonio Sica, and Frances Balkwill. Cancer-related inflammation. *Nature*, 454(7203):436–44, July 2008.

[109] Alberto Mantovani and Antonio Sica. Macrophages, innate immunity and cancer: balance, tolerance, and diversity. *Current Opinion in Immunology*, 22(2):231–237, April 2010.

[110] Alberto Mantovani, Antonio Sica, Silvano Sozzani, Paola Allavena, Annunciata Vecchi, and Massimo Locati. The chemokine system in diverse forms of macrophage activation and polarization. *Trends in Immunology*, 25(12):677–686, December 2004.

[111] Andriy Marusyk, Doris P. Tabassum, Philipp M. Altrock, Vanessa Almendro, Franziska Michor, and Kornelia Polyak. Non-cell-autonomous driving of tumour growth supports sub-clonal heterogeneity. *Nature*, 514(7520):54–58, October 2014.

[112] Lauren M F Merlo, John W Pepper, Brian J Reid, and Carlo C Maley. Cancer as an evolutionary and ecological process. *Nature reviews. Cancer*, 6(12):924–35, December 2006.

[113] Franziska Michor, Timothy P Hughes, Yoh Iwasa, Susan Branford, Neil P Shah, Charles L Sawyers, and Martin a Nowak. Dynamics of chronic myeloid leukaemia. *Nature*, 435(7046):1267–70, June 2005.

[114] Ron Milo, Paul Jorgensen, Uri Moran, Griffin Weber, and Michael

Springer. BioNumbers–the database of key numbers in molecular and cell biology. *Nucleic Acids Res*, 38(Database issue):D750–D753, January 2010.

[115] Shunichi Morikawa, Peter Baluk, Toshiyuki Kaidoh, Amy Haskell, Rakesh K. Jain, and Donald M. McDonald. Abnormalities in pericytes on blood vessels and endothelial sprouts in tumors. *The American Journal of Pathology*, 160(3):985–1000, March 2002.

[116] Gopal Murugaiyan and Bhaskar Saha. Protumor vs antitumor functions of IL-17. *J Immunol*, 183(7):4169–4175, October 2009.

[117] Carey D Nadell, Kevin R Foster, and João B Xavier. Emergence of spatial structure in cell groups and the evolution of cooperation. *PLoS computational biology*, 6(3):e1000716, January 2010.

[118] Larry Norton. A gompertzian model of human breast cancer growth. *Cancer research*, pages 7067–7071, 1988.

[119] P. C. Nowell. The clonal evolution of tumor cell populations. *Science*, 194(4260):23–28, October 1976.

[120] Satoshi Ohno, Nobutaka Suzuki, Yumiko Ohno, Hiroyuki Inagawa, Gen-Ichiro Soma, and Masaki Inoue. Tumor-associated macrophages: foe or accomplice of tumors? *Anticancer Res.*, 23(6a):4395–4409, December 2003.

[121] Shizue Ohsawa, Yoshitaka Sato, Masato Enomoto, Mai Nakamura, Aya Betsumiya, and Tatsushi Igaki. Mitochondrial defect drives non-autonomous tumour progression through hippo signalling in drosophila. *Nature*, 490(7421):547–551, September 2012.

[122] A Okubo. Dynamical aspects of animal grouping: swarms, schools, flocks, and herds. *Advances in biophysics*, 22:1–94, January 1986.

[123] Oakley C. Olson and Johanna A. Joyce. Microenvironment-mediated resistance to anticancer therapies. *Cell Res*, 23(2):179–181, February 2013.

[124] Akira Orimo, Piyush B Gupta, Dennis C Sgroi, Fernando Arenzana-Seisdedos, Thierry Delaunay, Rizwan Naeem, Vincent J Carey, Andrea L Richardson, and Robert a Weinberg. Stromal fibroblasts present in invasive human breast carcinomas promote tumor growth and angiogenesis through elevated SDF-1/CXCL12 secretion. *Cell*, 121(3):335–48, May 2005.

[125] Sarah P. Otto. *A biologist's guide to mathematical modeling in ecology and evolution*. Princeton University Press, Princeton, 2007.

[126] Markus R. Owen, Tomás Alarcón, Philip K. Maini, and Helen M. Byrne. Angiogenesis and vascular remodelling in normal and cancerous tissues. *J Math Biol*, 58(4-5):689–721, April 2009.

[127] Gergely Palla, Albert-László Barabási, and Tamás Vicsek. Quantifying social group evolution. *Nature*, 446(7136):664–7, April 2007.

[128] Chana Palmer, Maximilian Diehn, Ash A. Alizadeh, and Patrick O. Brown. Cell-type specific gene expression profiles of leukocytes in human peripheral blood. *BMC Genomics*, 7(1):115, May 2006.

[129] Y. Albert Pan, Tom Freundlich, Tamily A. Weissman, David Schoppik, X. Cindy Wang, Steve Zimmerman, Brian Ciruna, Joshua R. Sanes, Jeff W. Lichtman, and Alexander F. Schier. Zebrabow: multispectral cell labeling for cell tracing and lineage analysis in zebrafish. *Development*, 140(13):2835–2846, July 2013.

[130] Anoop P. Patel, Itay Tirosh, John J. Trombetta, Alex K. Shalek, Shawn M. Gillespie, Hiroaki Wakimoto, Daniel P. Cahill, Brian V. Nahed, William T. Curry, Robert L. Martuza, David N. Louis, Orit Rozenblatt-Rosen, Mario L. Suvà, Aviv Regev, and Bradley E. Bernstein. Single-cell RNA-seq highlights intratumoral heterogeneity in primary glioblastoma. *Science*, 344(6190):1396–1401, June 2014.

[131] Kornelia Polyak, Izhak Haviv, and Ian G Campbell. Co-evolution of tumor cells and their microenvironment. *Trends in genetics : TIG*, 25(1):30–8, January 2009.

[132] William H. Press, editor. *Numerical recipes: the art of scientific computing*. Cambridge University Press, Cambridge, UK ; New York, 3rd ed edition, 2007.

[133] Stephanie M Pyonteck, Leila Akkari, Alberto J Schuhmacher, Robert L Bowman, Lisa Sevenich, Daniela F Quail, Oakley C Olson, Marsha L Quick, Jason T Huse, Virginia Teijeiro, Manu Setty, Christina S Leslie, Yoko Oei, Alicia Pedraza, Jianan Zhang, Cameron W Brennan, James C Sutton, Eric C Holland, Dylan Daniel, and Johanna a Joyce. CSF-1r inhibition alters macrophage polarization and blocks glioma progression. *Nature medicine*, (August):1–12, September 2013.

[134] Bin-Zhi Qian and Jeffrey W Pollard. Macrophage diversity enhances tumor progression and metastasis. *Cell*, 141(1):39–51, April 2010.

[135] Daniela F. Quail and Johanna A. Joyce. Microenvironmental regulation of tumor progression and metastasis. *Nat Med*, 19(11):1423–1437, November 2013.

[136] Benjamin Ribba, Emmanuel Watkin, Michel Tod, Pascal Girard, Emmanuel Grenier, Benoît You, Enrico Giraudo, and Gilles Freyer. A model of vascular tumour growth in mice combining longitudinal tumour size data with histological biomarkers. *European Journal of Cancer*, 47(3):479–490, February 2011.

[137] Jeremy N Rich and Shideng Bao. Chemotherapy and cancer stem cells. *Cell stem cell*, 1(4):353–5, October 2007.

[138] Pawel Romanczuk, Iain Couzin, and Lutz Schimansky-Geier. Collective motion due to individual escape and pursuit response. *Physical Review Letters*, 102(1):1–4, January 2009.

[139] Pernille Rørth. Collective cell migration. *Annual review of cell and developmental biology*, 25:407–29, January 2009.

[140] Evanthia T Roussos, Michele Balsamo, Shannon K Alford, Jeffrey B Wyckoff, Bojana Gligorijevic, Yarong Wang, Maria Pozzuto, Robert Stobezki, Sumanta Goswami, Jeffrey E Segall, Douglas a Lauffenburger, Anne R Bresnick, Frank B Gertler, and John S Condeelis. Mena invasive (MenaINV) promotes multicellular streaming motility and transendothelial migration in a mouse model of breast cancer. *Journal of cell science*, 124(Pt 13):2120–31, July 2011.

[141] Jeffery S. Russell and J. Martin Brown. The irradiated tumor microenvironment: role of tumor-associated macrophages in vascular recovery. *Front. Physiol*, 4:157, 2013.

[142] Ruth Scherz-Shouval, Sandro Santagata, Marc L. Mendillo, Lynette M. Sholl, Irit Ben-Aharon, Andrew H. Beck, Dora Dias-Santagata, Martina Koeva, Salomon M. Stemmer, Luke Whitesell, and Susan Lindquist. The reprogramming of tumor stroma by HSF1 is a potent enabler of malignancy. *Cell*, 158(3):564–578, July 2014.

[143] Allyson E. Sgro, David J. Schwab, Javad Noorbakhsh, Troy Mestler,

Pankaj Mehta, and Thomas Gregor. From intracellular signaling to population oscillations: Bridging scales in collective behavior. *arXiv:1406.6731 [physics, q-bio]*, June 2014. arXiv: 1406.6731.

[144] Malgorzata Sielska, Piotr Przanowski, Bartosz Wylot, Konrad Gabrusiewicz, Marta Maleszewska, Magdalena Kijewska, Malgorzata Zawadzka, Joanna Kucharska, Katyayni Vinnakota, Helmut Kettenmann, Katarzyna Kotulska, Wieslawa Grajkowska, and Bozena Kaminska. Distinct roles of CSF family cytokines in macrophage infiltration and activation in glioma progression and injury response. *J. Pathol.*, 230(3):310–321, July 2013.

[145] Monica Simeoni, Paolo Magni, Cristiano Cammia, Giuseppe De Nicolao, Valter Croci, Enrico Pesenti, Massimiliano Germani, Italo Poggesi, and Maurizio Rocchetti. Predictive pharmacokinetic-pharmacodynamic modeling of tumor growth kinetics in xenograft models after administration of anticancer agents. *Cancer Res*, 64(3):1094–1101, February 2004.

[146] Dominic J. Smiraglia, Laura J. Rush, Michael C. Frühwald, Zunyan Dai, William A. Held, Joseph F. Costello, James C. Lang, Charis Eng, Bin Li, Fred A. Wright, Michael A. Caligiuri, and Christoph Plass. Excessive CpG island hypermethylation in cancer cell lines versus primary human malignancies. *Hum. Mol. Genet.*, 10(13):1413–1419, June 2001.

[147] Ricard V. Sole. *Phase Transitions*. Princeton University Press, Princeton, 2011.

[148] Richard R. Stein, Vanni Bucci, Nora C. Toussaint, Charlie G. Buffie, Gunnar Rätsch, Eric G. Pamer, Chris Sander, and João B. Xavier. Ecological modeling from time-series inference: Insight into dynamics and stability of intestinal microbiota. *PLoS Comput Biol*, 9(12):e1003388, December 2013.

[149] A Szabó, R Ünnep, E Méhes, WO Twal, SW Argraves, Y Cao, and A Czirók. Collective cell motion in endothelial monolayers. *Physical Biology*, 7(4), 2010.

[150] B. Szabó, GJ Szöllösi, B. Gönci, Z. Jurányi, D. Selmeczi, and T. Vicsek. Phase transition in the collective migration of tissue cells: experiment and model. *Physical Review E*, 74(6):061908, 2006.

[151] D.T. Tambe, C.C. Hardin, Thomas E. Angelini, Kavitha Rajendran, C.Y. Park, X. Serra-Picamal, E.H. Zhou, M.H. Zaman, J.P. Butler, D.A. Weitz,

Jeffrey J. Fredberg, and Xavier Trepat. Collective cell guidance by cooperative intercellular forces. *Nature Materials*, 10(6):469–475, 2011.

[152] John Toner and Yuhai Tu. Flocks, herds, and schools: A quantitative theory of flocking. *Physical Review E*, 58(4):4828–4858, October 1998.

[153] Binh-An Truong Quang, Madhav Mani, Olga Markova, Thomas Lecuit, and Pierre-François Lenne. Principles of e-cadherin supramolecular organization in vivo. *Current Biology*, 23(22):2197–2207, November 2013.

[154] Dave van Ditmarsch, Kerry E. Boyle, Hassan Sakhtah, Jennifer E. Oyler, Carey D. Nadell, Éric Déziel, Lars E. P. Dietrich, and Joao B. Xavier. Convergent evolution of hyperswarming leads to impaired biofilm formation in pathogenic bacteria. *Cell Reports*, 4(4):697–708, August 2013.

[155] Peter Vaupel. Tumor microenvironmental physiology and its implications for radiation oncology. *Seminars in Radiation Oncology*, 14(3):198–206, July 2004.

[156] T. Vicsek, A. Czirók, Eshel Ben-Jacob, I. Cohen, and O. Shochet. Novel type of phase transition in a system of self-driven particles. *Physical Review Letters*, 75(6):1226–1229, 1995.

[157] Tamás Vicsek and Anna Zafeiris. Collective motion. *arXiv*, pages 1–85, 2012.

[158] Joe Yuichiro Wakano, Martin a Nowak, and Christoph Hauert. Spatial dynamics of ecological public goods. *Proceedings of the National Academy of Sciences of the United States of America*, 106(19):7910–4, May 2009.

[159] Richard Mark White, Anna Sessa, Christopher Burke, Teresa Bowman, Jocelyn LeBlanc, Craig Ceol, Caitlin Bourque, Michael Dovey, Wolfram Goessling, Caroline Erter Burns, and Leonard I. Zon. Transparent adult zebrafish as a tool for in vivo transplantation analysis. *Cell Stem Cell*, 2(2):183–189, February 2008.

[160] K. P. Wilkie and P. Hahnfeldt. Mathematical models of immune-induced cancer dormancy and the emergence of immune evasion. *Interface Focus*, 3(4):20130010–20130010, June 2013.

[161] Michael J. Wiser, Noah Ribeck, and Richard E. Lenski. Long-term dynam-

ics of adaptation in asexual populations. *Science*, 342(6164):1364–1367, December 2013.

[162] Adam Wu, Jun Wei, Ling-Yuan Kong, Yongtao Wang, Waldemar Priebe, Wei Qiao, Raymond Sawaya, and Amy B. Heimberger. Glioma cancer stem cells induce immunosuppressive macrophages/microglia. *Neuro Oncol*, 12(11):1113–1125, November 2010.

[163] Ming Wu, José Carlos Pastor-Pareja, and Tian Xu. Interaction between ras(v12) and scribbled clones induces tumour growth and invasion. *Nature*, 463(7280):545–8, January 2010.

[164] Jeffrey Wyckoff, W Wang, EY Lin, Yarong Wang, Fiona Pixley, and ER. A paracrine loop between tumor cells and macrophages is required for tumor cell migration in mammary tumors. *Cancer research*, pages 7022–7029, 2004.

[165] Jeffrey B Wyckoff, Joan G Jones, John S Condeelis, and Jeffrey E Segall. A critical step in metastasis : In vivo analysis of intravasation at the primary tumor a critical step in metastasis : In vivo analysis of intravasation at the. *Cancer Research*, pages 2504–2511, 2000.

[166] Jeffrey B Wyckoff, Yarong Wang, Elaine Y Lin, Jiu-feng Li, Sumanta Goswami, E Richard Stanley, Jeffrey E Segall, Jeffrey W Pollard, and John Condeelis. Direct visualization of macrophage-assisted tumor cell intravasation in mammary tumors. *Cancer research*, 67(6):2649–56, March 2007.

[167] K. K. Yan, G. Fang, N. Bhardwaj, R. P. Alexander, and M. Gerstein. Comparing genomes to computer operating systems in terms of the topology and evolution of their regulatory control networks. *Proceedings of the National Academy of Sciences*, May 2010.

[168] Jianjun Zhang, Junya Fujimoto, Jianhua Zhang, David C. Wedge, Xingzhi Song, Jiexin Zhang, Sahil Seth, Chi-Wan Chow, Yu Cao, Curtis Gumbs, Kathryn A. Gold, Neda Kalhor, Latasha Little, Harshad Mahadeshwar, Cesar Moran, Alexei Protopopov, Huandong Sun, Jiabin Tang, Xifeng Wu, Yuanqing Ye, William N. William, J. Jack Lee, John V. Heymach, Waun Ki Hong, Stephen Swisher, Ignacio I. Wistuba, and P. Andrew Futreal. Intratumor heterogeneity in localized lung adenocarcinomas delineated by multiregion sequencing. *Science*, 346(6206):256–259, October 2014.

[169] Jing Zhang, Susobhan Sarkar, Rowena Cua, Yan Zhou, Walter Hader, and

V. Wee Yong. A dialog between glioma and microglia that promotes tumor invasiveness through the CCL2/CCR2/interleukin-6 axis. *Carcinogenesis*, 33(2):312–319, February 2012.

[170] Le Zhang, Zhihui Wang, Jonathan a Sagotsky, and Thomas S Deisboeck. Multiscale agent-based cancer modeling. *Journal of mathematical biology*, 58(4-5):545–59, April 2009.